

**Copine 6, a novel calcium sensor  
translating  
synaptic activity into spine plasticity.**

or

“Copine 6 a brainsporter in action”

**Inauguraldissertation**

zur

Erlangung der Würde eines Doktors der Philosophie

vorgelegt der

Philosophisch-Naturwissenschaftlichen Fakultät

der Universität Basel

von

**Alexander Kriz**

aus Wien, Österreich

**Biozentrum der Universität Basel**

**Basel, März 2010**

Genehmigt von der Philosophisch-Naturwissenschaftlichen Fakultät auf Antrag von

**Prof. Dr. Markus A. Rüegg**

**Prof. Dr. Bernhard Bettler**

**Basel, den 08/12/2009**

**Prof. Dr. Eberhard Parlow**  
**Dekan**

***The structure of consciousness***

**“The interaction and interference of multiple brain rhythms often gives rise to the appearance of ‘noise’ in an electroencephalogram. This noise is the most complex type known to physics and reflects a metastable state between the predictable behaviour of oscillators and the unpredictability of chaos”**

György Buzsáki,

***Nature Essay /Vol 446/15 March 2007***

When I read this statement first time during the initial phase of my study I wanted to know how exactly an electroencephalogram works, how an oscillator oscillates and wondered about the possibility of things existing in a metastable state. However after 4 years of studying with endless nights of analyzing neurons, hours of cloning and avoiding forgetting any food in the Department fridge, I best of all learned what chaos means. And believe me it is predictable.

The Author

---

## Table of content

<b>Summary .....</b>	<b>6</b>
<b>Introduction (general).....</b>	<b>7</b>
<b>The CNS synapse.....</b>	<b>8</b>
Synaptic architecture .....	8
Synaptogenesis .....	10
Synaptic transmission.....	11
Synaptic plasticity .....	13
<b>Small GTPases and their role in spine maturation.....</b>	<b>14</b>
Switching between GDP and GTP.....	14
Synaptic activity and Rac1 GTPase responses.....	15
<b>Copines .....</b>	<b>17</b>
An overview .....	17
Copine 6 what is known so far.....	18
<b>Summary (manuscript).....</b>	<b>21</b>
<b>Introduction (manuscript).....</b>	<b>22</b>
<b>Results.....</b>	<b>24</b>
Timepoint of synapse formation in primary hippocampal neurons .....	24
Copine 6 expression and location in the CNS.....	25
Copine 6 binds reversibly to the Plasma Membrane in a calcium dependent manner .....	27
Copine 6 affinity to plasma membranes is strengthened by cholesterol rich domains.....	28
Ca <sup>2+</sup> dependent enrichment of Copine 6 in PSDs.....	29
NMDAR mediated Copine 6 translocation.....	30
Loss of Copine 6 increases $\beta$ -actin positive protrusion density.....	31
Loss of Copine 6 increases synaptic density.....	33
Overexpression of Copine 6 has no effect on neuronal morphology or synaptic transmission....	35
A calcium blind Copine 6 mutant causes spine loss and an increase in filopodia .....	36
Copine 6 recruits the small Rho like GTPase Rac1 to the membrane in a calcium dependent manner.....	37
<b>Discussion .....</b>	<b>40</b>
Copine 6 expression indicates a postsynaptic function.....	40
Calcium triggers translocation of Copine 6 to lipid rafts .....	40

---

Copine 6 translates synaptic activity to spine stability.....	41
Copine 6 regulates synapse number via Rac1.....	42
<b>Materials and Methods .....</b>	<b>44</b>
DNA constructs and antibodies .....	44
Quantitative real-time PCR.....	44
Pharmacological agents and inhibitors.....	45
Primary hippocampal cultures .....	45
Transfection, Immunocytochemistry.....	45
Ionomycin treatment .....	46
Lipid raft staining.....	46
Imaging .....	46
Cholesterol depletion .....	46
Lipid raft isolation .....	46
Subcellular fractionation of COS7 cells .....	47
PSD fractionation and isolation of rat brains .....	47
Life imaging.....	48
Electrophysiology.....	48
Two-photon laser imaging .....	49
Immunoprecipitation and Western blotting .....	49
Crosslinking .....	49
<b>References .....</b>	<b>51</b>
<b>Acknowledgement.....</b>	<b>57</b>
<b>Curriculum Vitae:.....</b>	<b>58</b>

---

## Summary

Changes in synaptic activity alter synaptic transmission, ultimately changing neuronal network dynamics. Importantly, shifting synaptic properties often induces calcium-dependent structural rearrangements. The consequence of activity-dependent influx of calcium has been well studied and many of its targets have emerged over the last years. However, most of these studies are emphasizing the interaction of these proteins but ignore mechanisms controlling its spatio-temporal properties. Here we introduce a novel mechanism for activity dependent synapse plasticity based on protein translocation. We were able to demonstrate increased synaptic activity upon loss of Copine 6 in hippocampal neurons and show its enrichment in postsynaptic compartments upon NMDA receptor dependent calcium influx. Moreover, we show evidence for Copine 6 acting as a shuttle protein for the small Rho-like GTPase Rac1. In the presence of Copine 6, Rac1 shows calcium dependent enrichment at cell membranes. Interestingly neurons expressing a calcium-insensitive version of Copine 6 lose active synapses. Together, these data provide evidence that Copine 6 translates synaptic activity into morphological changes through translocation of Rac1 into synaptic structures in a calcium-dependent manner.

---

## Introduction (general)

The most complex organ in the human body is the brain. No other organ is so little described and is subject of so many assumptions, speculations and theories. Through the brain we interact with our environment. We are able to process all main sensory information, which after the final assembly has taken place, gives rise to the world how we experience it. Its enormous processing power coupled with the possibility to integrate all kinds of different, more or less linked, information contents (creativity) results in a wide spectrum of abilities. From composing a symphony to the development and construction of devices which can not only escape our planets gravitation but even leave our solar system. We are just beginning to understand our brain in its very fundamental functions. To understand how we learn and memorize, the focus has to be relocated from the brain as a whole organ to a much higher resolution to one of the building blocks of our brain, the neurons. In no other tissue, cells are linked with each other in such a complex and dense way. This creation of neuronal circuits allows the exchange and propagation of information in the form of electricity. The same principle of information processing can be found in such a complex way only in modern computer chip technology. To achieve this enormous processing power, the brain uses the biggest strength neurons have, the ability of acting in concert. In a simplified way, the main function of a neuron can be considered as a capacitor creating a voltage difference due to an imbalance of positively and negatively charged ions across the cell membrane. Ion channels link these two compartments and the actual information is then transmitted as a short change in that charge, mediated by a short opening of the ion channels. To transmit the information from one cell to another a highly specialized structure is needed; the synapse.

## The CNS synapse

A synapse in the central nervous system (CNS) is the connection between two neurons. It can be roughly described as being composed of a source unit like a speaker, creating an output from one cell and tightly coupled to it a microphone device from a second cell which is receiving the information from the first cell. The combined structure of this source unit (presynapse) and receiving unit (postsynapse) gives rise to the synapse itself which in the end links two individual cells to a network. This type of cell – cell connection ensures that one cell can interact with many other (individual) cells, without losing the individual properties of each single synapse. To achieve a good connection between two cells the presynapse has to be linked to the postsynapse via adhesion molecules. Losing connectivity would also mean to lose the ability to transmit information, so neurons developed a whole subset of molecules involved in cell-cell contact which strengthen the fragile synaptic structure.

### Synaptic architecture

In the central nervous system two different kinds of synapses are known; electrical (**Fig. 1A, left**) and chemical synapses (**Fig. 1B, right**). While electrical synapses are directly linked with each other and also outperform chemical synapses in terms of transmission speed, the majority of the synapses in the human brain are chemical synapses.

The direct linkage of the electrical synapse is mediated by specialized structures in the pre- and postsynaptic membrane.

These structures, called gap junction channels are hexameric complexes creating a pore in each partner's cell membrane, even wide enough for the diffusion of small proteins.

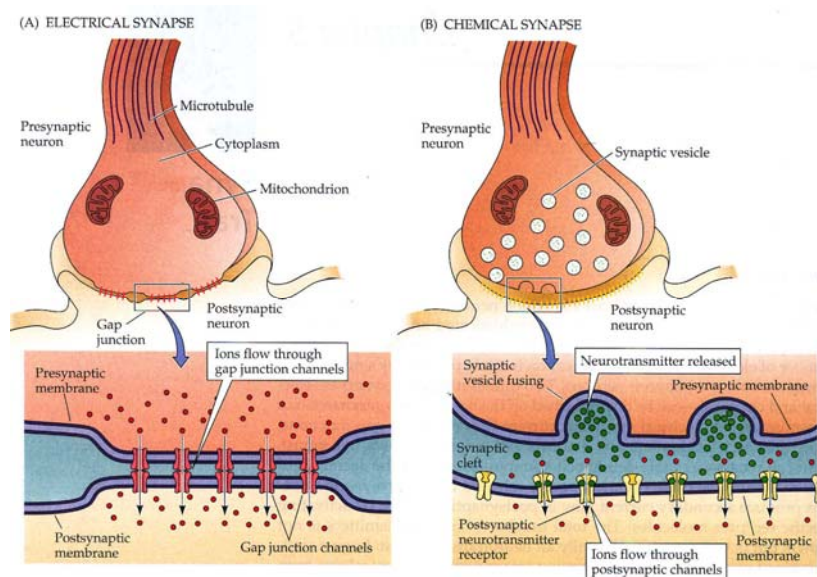


**Figure 1: Electrical and Chemical synapses**

(A) An electrical synapse, note the close proximity of the pre- and postsynapse which are linked via Gap junction channels. (B) In a chemical synapse the pre- and postsynapse are separated by the synaptic cleft. This requires a complex system composed of molecules involved in neurotransmitter release and neurotransmitter receptors receiving the chemical information (adapted from Purves D. Neuroscience, 3<sup>rd</sup> Edition).



Thus neurons with electrical synapses share their intracellular space causing a nearly instantaneous transmission of ions without delay. In brain regions such as the brainstem where a high level of synchrony in a neuronal network has to be achieved (e.g.: to govern breathing) these synapses are of vital importance. Chemical synapses in contrast are not linked via Gap junction channels. An axonal ending which contains the presynapse and the dendritic postsynapse are separated by a synaptic cleft. This architecture needs the formation of complex machineries which are able to span the synaptic cleft avoiding to lose information.

Basically these trans-synaptic protein interactions mediated by adhesion molecules stabilize and hence secure the synaptic entity (**Fig. 2**). So far a whole group of protein interactions were identified like Cadherin-Cadherin [1, 2],  $\beta$ -Neurexin-Neuroigin [3], SynCAM-SynCAM [4] and EphrinB-EphB receptor [5]. All these adhesion molecules are linked via scaffolding molecules (e.g. catenins, PSD-95 and CASK) to the two synaptic compartments, anchoring them at active synapses and these synapses themselves.

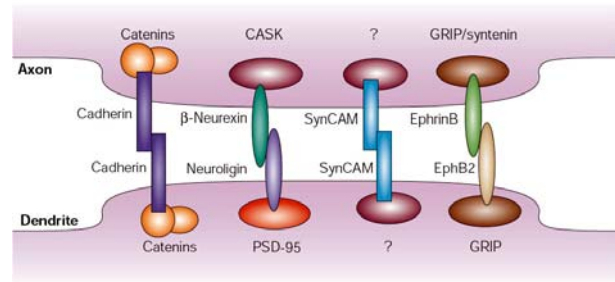


**Figure 2: The basic principle of adhesion molecules in synapses.** Cadherins are anchored to the synapse by Catenins while Neuroigin /  $\beta$ -Neurexins, SynCAMs and EphrinB / EphB2 receptors are anchored by PDZ domain containing proteins. SynCAMs can bind to a multitude of proteins containing PDZ domains, indicated with a question mark. CASK, protein containing  $\text{Ca}^{2+}$ /calmodulin-dependent-kinase, SH3 and guanylate-kinase domains; GRIP, glutamate-receptor-interacting protein; PSD95, postsynaptic-density protein of 95kDa. (adapted from Li et al. Nature Reviews Mol.Cel.Biol. Vol 4, 2003)

Additionally it was shown that certain adhesion molecules also serve as signaling receptors translating a contact into a signaling cascade, which influences the development and maturation of synapses [5] (see below). To further ensure a tightly regulated and reliable synaptic transmission, the presynaptic membrane gives rise to the active zone, an area determined for localized neurotransmitter exocytosis. At the exact opposite site the postsynaptic membrane presents the postsynaptic density a cluster of neurotransmitter receptors sensing the released neurotransmitter, localized by the insertion into an electron dense protein scaffold. This neurotransmitter, mainly the molecule glutamate mediates most excitatory neurotransmission and binds to certain glutamate receptors. Due to the fact that excitation will be one of the main processes presented here, synaptic inhibition will not be discussed despite its pivotal role in a balanced network activity. Glutamate receptors can be separated into ionotropic receptors, which act as simple ion channels and metabotropic receptors which are coupled to G proteins and link glutamate release to G protein-mediated signaling cascades [6]. Considering the following chapters to come, three postsynaptic proteins should be introduced here the two ionotropic receptors  *$\alpha$ -amino-3-hydroxy-5-methyl-4-isoxazole propionate receptor (AMPA)* the *N-methyl-D-aspartate receptor (NMDAR)* and

one member of the scaffolding proteins; the *postsynaptic density protein 95* (PSD95). The AMPAR is in comparison to the NMDAR an electrophysiologically rapidly responding receptor while the NMDAR is responsible for a slower phase of neurotransmission and needs the pre activation of AMPARs, to be opened by glutamate [7]. Both proteins are inserted into the postsynaptic density via certain scaffolding proteins [8]. Those create a lattice under the postsynaptic membrane, organizing receptors, signaling molecules, kinases and phosphatases at the synapse [9]. The protein PSD 95 is one of these scaffolding proteins. It binds directly to the NMDAR with its PSD95, Discs large, Zona occludens-1 (PDZ) domain, which is a protein-protein interaction motif, binding to short amino-acid sequences at the carboxyl-terminus of membrane proteins [10].

## Synaptogenesis

Most of the knowledge about synaptogenesis derives from the observation of dendritic spines. Since most excitatory synapses are located on spines in the mammalian brain [11] it becomes clear that understanding the formation of spines might also shed light on the process of synaptogenesis itself. The development of new technologies in the field of microscopy and life cell imaging, including the Two-Photon-Time-Lapse Microscopy combined with tracking the movement of fluorescently labeled marker proteins like PSD95 clearly showed that dendritic spines are highly dynamic structures changing their shape within a couple of minutes [12, 13]. The discovery that highly motile filopodia, thin actin rich structures, can give rise to mature spines and vice versa, as well as the fact that filopodia are most abundant only in the young brain but are replaced by spines in more mature stages, point to a filopodia – spine transition [14]. It is now widely accepted that dendritic filopodia are the precursors of dendritic spines. **Figure 3** summarizes the steps leading to synaptogenesis in a more descriptive chronology and in terms of protein kinetics.

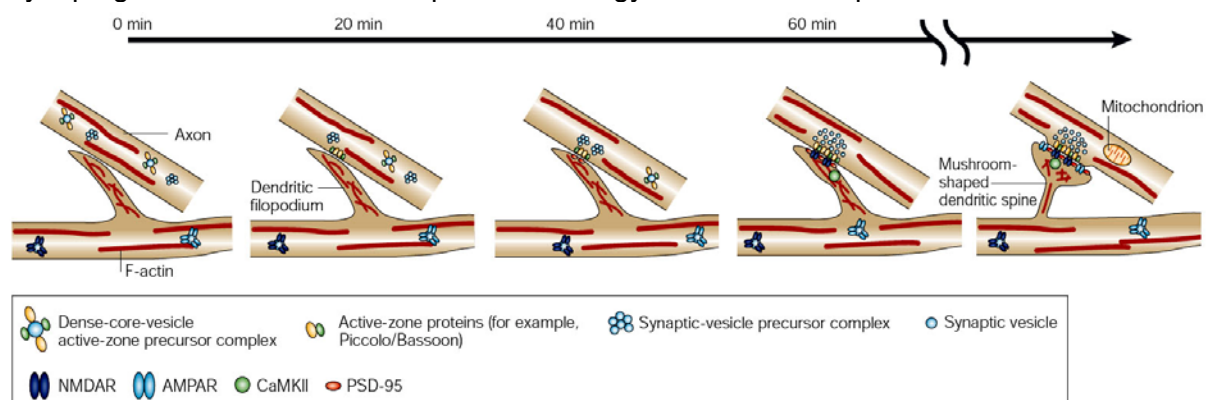


**Figure 3: The sequence of molecular and morphological events in synapse assembly and maturation.**

After the initial contact of a dendritic filopodium and an axon Bassoon and Piccolo, integrated into a “packet-like” dense-core-vesicle active-zone precursor complex are getting immobilized at the presynaptic site of the nascent synapse. They create a framework for recruiting further presynaptic residues like the synaptic-vesicle complex containing the main constituents of the synaptic vesicle release machinery. In parallel PSD95 one of the earliest present postsynaptic marker proteins and a main scaffold protein determines the putative postsynaptic density. After the development into a mature presynapse and the insertion of neurotransmitter receptors, first NMDAR then AMPAR the synapse matured to a fully functional entity. (adapted from Li et al. Nature Reviews Mol.Cel.Biol. Vol 4, 2003)

---

The first contact of an above described dendritic filopodium and an axon, results in the contact of adhesion molecules like neuroligin (**Fig. 2**). This contact initiates the recruitment of proteins which mark the now generated site of the nascent synapse. Some studies suggest an initial key role of the filopodium and its premature postsynapse in inducing the formation of the presynapse [15]. However, in hippocampal cultures the presynaptic markers Bassoon and Piccolo are the first proteins present at the putative synapse [16]. To ensure the high speed of synaptogenesis (the initial steps are accomplished within minutes) these proteins are delivered in “packages” which are freely diffusible in the axon but are immediately immobilized at nascent synapses, thus this provides a framework for the recruitment of further proteins [17]. The Bassoon/Piccolo complex is present before the rapid recruitment of the scaffold protein PSD95 happens, indicating that presynaptic differentiation precedes postsynaptic development. Nevertheless, not all synaptic markers are known and not all characterized markers have been tested so far for their spatial and temporal distribution in a synaptogenesis paradigm. Synapse associated protein 102 kDa (SAP-102) for example is present earlier in rat hippocampal PSDs than PSD95 [18]. Additionally, it was shown in young cortical neurons that the NMDAR is recruited within a few minutes after the initial dendritic and axonal contact [19] but in mature hippocampal neurons this recruitment takes a couple of hours (but is still preceding the AMPAR recruitment) [16]. Therefore it is not clear which synaptic site precedes the other or if indeed synaptogenesis is a continuous “crosstalk” of both the developing dendritic filopodium and the putative presynaptic bouton. Furthermore, synaptogenesis may be additionally influenced by different neuron types and ages. After the final synapse assembly, proteins like CaMKII are enriched at postsynaptic structures. CaMKII is involved in translating synaptic activity into a physiological response (see below).

### **Synaptic transmission**

As the neuron is inserted into its network it is constantly receiving excitatory and inhibitory inputs through its synapses. This can be measured as a small depolarization in case of an excitatory or hyperpolarization in case of an inhibitory signal. All these inputs are constantly integrated, which means that all events are summed up. If the sum of all inputs exceeds a certain depolarizing threshold, an action potential is generated at the axonal hillock, the site where the axon arises from the cell body. The axonal hillock is a place with a very high density of voltage gated sodium channels (VGSC). Once these channels are opened through the integrated, depolarizing signal, they cause an influx of sodium which depolarizes the next axonal stretch, causing again the opening of VGSCs. That is when an action potential is generated, which like a sodium wave, propagates down the axon. The events following the arrival of the action potential at the presynapse are shown in **Figure 4**.

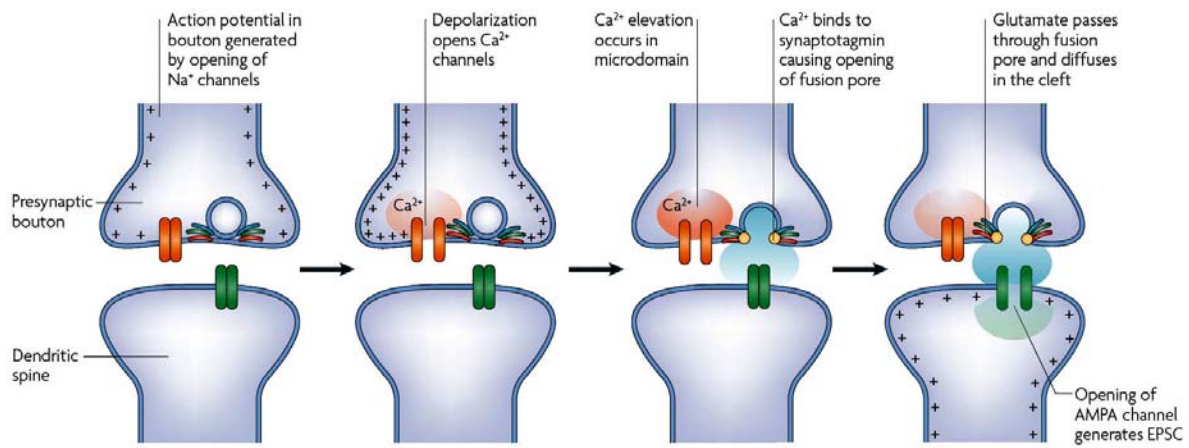


**Figure 4 Steps in the process of chemical synaptic transmission**

Opening of voltage dependent sodium channels inserted in the presynaptic membrane cause depolarization of the presynaptic bouton which opens voltage gated calcium channels. A local calcium influx (red) fuses synaptic vesicles with the active zone releasing glutamate (blue). Glutamate opens AMPAR which depolarizes the postsynapse by an influx of sodium ions (light green; adapted from Lisman et al. Nature Reviews Neuroscience 18Jul/2007).

The action potential arrives at the presynapse and causes a depolarization of voltage dependent calcium channels (VDCCs). Opening of these channels results in a local increase of calcium creating a microdomain of high calcium near the active zone of the presynapse [20, 21]. This calcium elevation initiates the fusion of synaptic vesicles which are docked at the active zone, with the active zone membrane (**Fig 5**).

This process is triggered by a subset of calcium sensing proteins like synaptotagmin, synaptobrevin and syntaxin (the SNARE complex) which are integrated into the synaptic vesicle membrane and the active zone membrane [22-24]. In the presence of calcium these proteins change their conformation and force a fusion of the presynaptic vesicles, filled with neurotransmitters (glutamate, glycine, GABA or acetylcholine), with the active zone membrane, finally causing a release of the vesicle interior into the synaptic cleft. The neurotransmitters diffuse across the narrow synaptic cleft and bind to neurotransmitter receptors like AMPAR; NMDAR, or GABAR depending on the nature of the neurotransmitter.

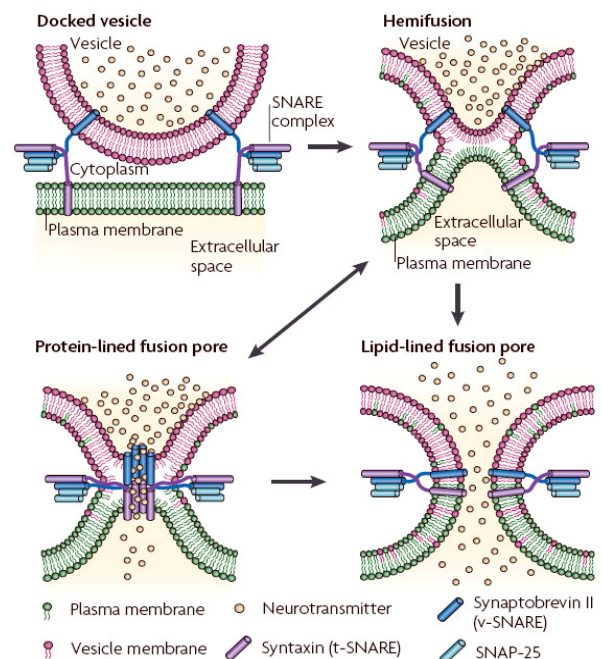


**Figure 5: Synaptic vesicle fusion and fusion pores**

(**top left**) the synaptic vesicle (pink) is “docked” to the plasma membrane (green) by the SNARE complex. Immediately before fusion occurs the vesicle is primed by hemifusion (**top right**). If the calcium concentration exceeds a certain level the synaptic membrane fuses completely with the plasma membrane (**bottom right**) that might involve also the SNARE complex itself in certain transition states (**bottom left**). Total fusion will lead to a release of neurotransmitter into the synaptic cleft.

(adapted from Lisman et al. Nature Reviews Neuroscience 18Jul/2007).

Opening of e.g. AMPAR creates a sodium influx into the neuron which causes a depolarization of the membrane in the near vicinity. This depolarization can be measured as an Excitatory Postsynaptic Current (EPSC) which renders a second neurotransmitter receptor, the NMDAR, sensitive for glutamate via the release of its magnesium block. Removal of this block finally results in the influx of even more sodium and importantly of calcium through the NMDA receptor. These events further depolarize the cell and influence local synaptic calcium sensing proteins. If the integrated activation of all synapses exceeds a certain threshold, a new action potential is formed at the axonal hillock, which propagates down the axon.

## Synaptic plasticity

A remarkable hallmark of synapses is their possibility to adapt to their level of usage. A heavily used synapse has a different morphology than a nearly unused one (**Fig 6**).

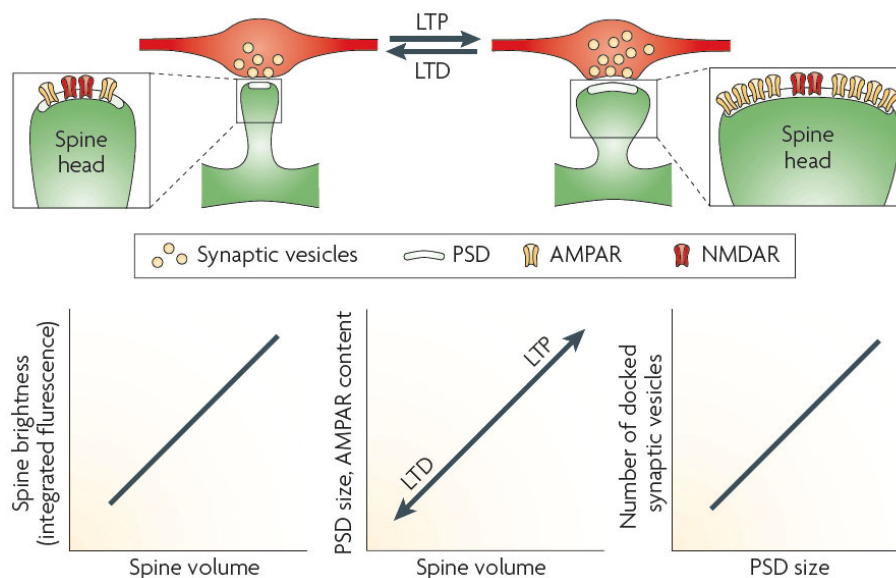


**Figure 6: Correlates of synaptic strength**

It is a well accepted fact that measuring spine volume provides an excellent indication for synaptic strength. An increase in spine volume is proportional to an increase in PSD area which in turn is proportional to AMPAR density and to postsynaptic glutamate sensitivity. Furthermore the PSD size correlates with presynaptic parameters like docked vesicles and the quality of synaptic vesicle fusion. (adapted from Holtmaat A. et al. Nature Reviews Neuroscience Vol 10 / Sept 2007)

The phenomenon of strengthening and weakening of synaptic contacts by activity is known as synaptic plasticity [25]. Long term potentiation (LTP) for example describes the strengthening and growth of a synapse, while Long term depression (LTD) refers to the weakening and shrinking of the synapse. These two mechanisms are best thought to describe the molecular machinery underlying learning and memory [26, 27]. LTP possesses the possibility to link neuronal networks and consolidate the synaptic contacts in this circuit. It basically takes care of the further existence of these connections, simply because they are used, which means they are needed. LTD describes the initial weakening of synaptic connections eventually followed by their break down and finally the loss of particular

---

synapses [28, 29]. On the molecular level LTP and LTD can be described as an enrichment (LTP) or removal (LTD) of AMPAR at the PSD [30-32]. This effect seems to be mainly governed by the NMDAR mediated calcium influx as NMDAR inhibitors also inhibit LTP formation [33]. Elevated calcium levels on the other hand are sensed by certain calcium binding molecules, like calmodulin which in turn leads to the activation of the calmodulin dependent kinase II (CaMKII). This kinase is one of the most abundant proteins in the CNS. Its activation causes a translocation into the postsynaptic compartment [34]. There it is involved in the rearrangement of the actin cytoskeleton and in the stabilization of AMPARs via the phosphorylation of special sites at their c-terminal part [35]. The events taking place at the presynapse when LTP occurs are harder to monitor, but recent studies describe a correlation of LTP protocols and the amount of glutamate in the synaptic cleft. Interestingly, this increase is not due to an elevation of the number of synaptic vesicles fusing with the active zone. Instead it is triggered by an increase of the fusion pore generated by single vesicles unloading their content. This implies a “super primed” mode of the SNARE complex causing a higher release of glutamate [36, 37]. The analysis of the chronologic sequence of events in the postsynapse underlying the LTP process, revealed that in the first few minutes the consistent actin turnover is slowed down by a decrease in the activity of actin depolymerizing enzymes, like cofilin [38-40]. This causes an enrichment of polymerized actin filaments in the spine, which finally causes the increase in spine volume and in parallel spine surface. This increased surface is accompanied with an increase in the underlying PSD scaffold, which creates space for additional AMPARs [41, 42]. A high density of AMPARs can be clearly visualized as an increase in synaptic ion flux. The presynaptic neurotransmitter release can activate more receptors which in turn will cause a bigger influx of cations into the intracellular space therefore causing a bigger depolarization of the neuron.

## **Small GTPases and their role in spine maturation**

### **Switching between GDP and GTP**

Among all tissues in the mammalian body, neurons belong to the most specialized cell types. Their high degree of complexity and their need to project long distances (sometimes spanning a meter) can be only achieved by a subset of molecules; the small Rho like GTPases involved in cell polarization [43]. These polarizing mechanisms generate the individual neuronal compartments like dendrites, axons, axonal boutons and spines and determine their final shape, stability and with that their functionality [44]. In compartments of



high plasticity like spines, these molecules have to quickly adapt to a fast changing environment. This explains their basic biochemical properties as molecular switches. They can be either turned on or off in a rather fast and reliable way depending on inductive signals derived from the environment. **Figure 7** summarizes the main events involved in such a switching process.

To allow a tight regulation temporally and spatially, Rho GTPases have the ability for low intrinsic GTP hydrolysis.

Furthermore, specific GTPase activating proteins (GAPs) enhance the inactivation reaction, providing the cell with the opportunity to control the degree of Rho GTPase silencing. In the inactive, GDP-bound state, Rho GTPases can be mainly found in the cytosol. This sequestration is further strengthened via guanine nucleotide dissociation inhibitors (GDIs). These proteins bind and block the c-terminus of the GTPases, which is required for their interaction with phospholipids. Only in combination with the dissociation of GDIs and the activation of the particular GTPases mediated through guanine nucleotide exchange factors (GEFs) like Tiam-1, Kalirin-7 or  $\beta$ PIX causes the translocation to the membrane and the replacement of GDP with GTP.

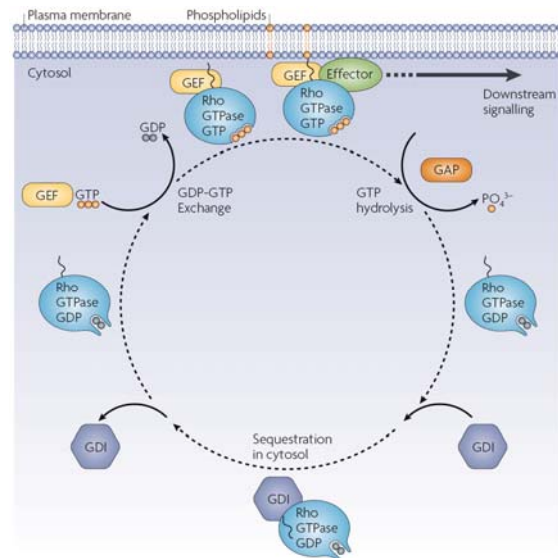


**Figure 7: Rho family GTPases and their regulators** (clockwise from top) activated GTP bound GTPases have an intrinsic increased affinity to the plasma membrane due to palmitoylation at the c-terminus. Effector molecules translate the activation into a downstream signalling. GAP proteins hydrolyse GTPases to the inactive GDP state and GDIs further sequester GTPases into the cytosol by blocking their c-terminus. GEF molecules facilitate the GDP to GTP switch causing the activation of GTPases. GAP; GTPase activating protein; GDI, guanine nucleotide-dissociation inhibitor; GEF, guanine nucleotide-exchange factor. (adapted from Iden S et. al Nature Reviews Mol.Cel.Biol. Vol 9 / 2008)

The activated GTPases further activate numerous downstream effectors like p21 activated kinase 1 (PAK1) and the WAVE/WASP complex which translate the GTPase transition into a physiological reaction (actin remodeling, microtubule capture, cell-cell adhesion, induction of gene expression) [45].

### Synaptic activity and Rac1 GTPase responses

The dependency of actin regulation on synaptic activity is a widely studied field. One signal module based on CaMKII, shows key functions in translating high frequency synaptic activity into the stabilization of actin filaments (**blue arrows Fig. 8**) [46, 47]. In dendritic spines, synaptic activity causes NMDA receptor mediated elevation of intrasynaptic calcium levels. Depending on the quality of this elevation either strengthening or weakening of synapses occurs (see LTP/LTD part). Strengthening of synapses basically involves the activation of

CaMKII-mediated activation of the CaMKK-CaMKI signaling pathway [48]. These kinases form a multimolecular complex with the Rac1-specific guanosine exchange factor  $\beta$ PIX. Calcium induced activation of CaMKII increases the GEF activity of  $\beta$ PIX, which causes a further activation of the Rho GTPase Rac1 [49, 50]. Activated Rac1 triggers the autophosphorylation and activation of p21-activated-kinase 1 (PAK1), which also interacts with  $\beta$ PIX. Pak1 is the major activator of the LIM kinase (LIMK) which inhibits the actin destabilizing ADF/Cofilin protein family [39].

Inhibition of ADF/Cofilin maintains actin fibers and stabilizes synaptic structures. Interestingly Rac1 can also be directly activated by CaMKII via the GEF molecule Kalirin-7 bypassing the CaMKK-CaMKI signaling cascade. A second, Rac1-independent pathway that stabilizes actin fibers involves the RhoA GTPase. It interacts directly with the NMDA receptor in an activity dependent manner. Activation of RhoA causes activation of Profilin II, an actin-binding protein, via the RhoA-specific kinase (ROCK) [51, 52]. In case of a low frequency synaptic stimulation which induces long lasting, but low concentrated, calcium elevations, CaMKII is not activated (red arrows Fig. 8). Nevertheless the phosphatase Calcineurin turns on the ADF/Cofilin family proteins which leads to a localized depolymerization of actin fibers and a subsequent destabilization of spine structures [29].

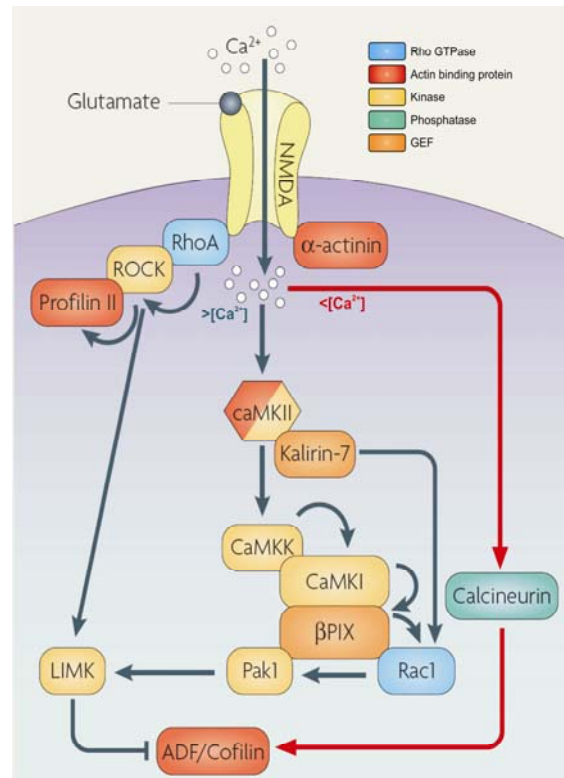


**Figure 8: Actin signaling in dendritic spines**  
NMDAR derived calcium influx mediated by repetitive synaptic stimulation (blue arrows) activates CaMKII and further downstream effectors involving the small Rho-like GTPase Rac1 subsequently causing the polymerization and stabilization of actin fibers. Low frequency stimulation of the NMDAR (red arrows) activates calcineurin which activates actin depolymerizing molecules inducing the shrinking and final break down of synaptic structures. (modified from Cingolani L. et al. Nature Reviews Vol 9 / 2008).



# Copines

## An overview

The members of the Copine family are a scarcely described group of cytosolic proteins. Their amino acid sequence shows a high degree of similarity between all kinds of organisms from *Paramecium* to *Homo sapiens*. In mammals the so far known eight family members have a mass of 60kDa. Their highly conserved architecture contains a pair of calcium sensing C2 domains at the N-terminus, followed by a domain, similar to the A domain that mediates interactions between integrins and extracellular ligands. The C-terminus however is highly divergent probably conferring unique characteristics to each family member (**Fig. 9A**). Copines have been first described as calcium sensing protein in *Paramecium tetraurelia* which increase their affinity to phospholipids upon the elevation of intracellular calcium [53]. This calcium-dependent response is regulated by the above described C2A and C2B domains, which are conserved calcium sensing modules [54].

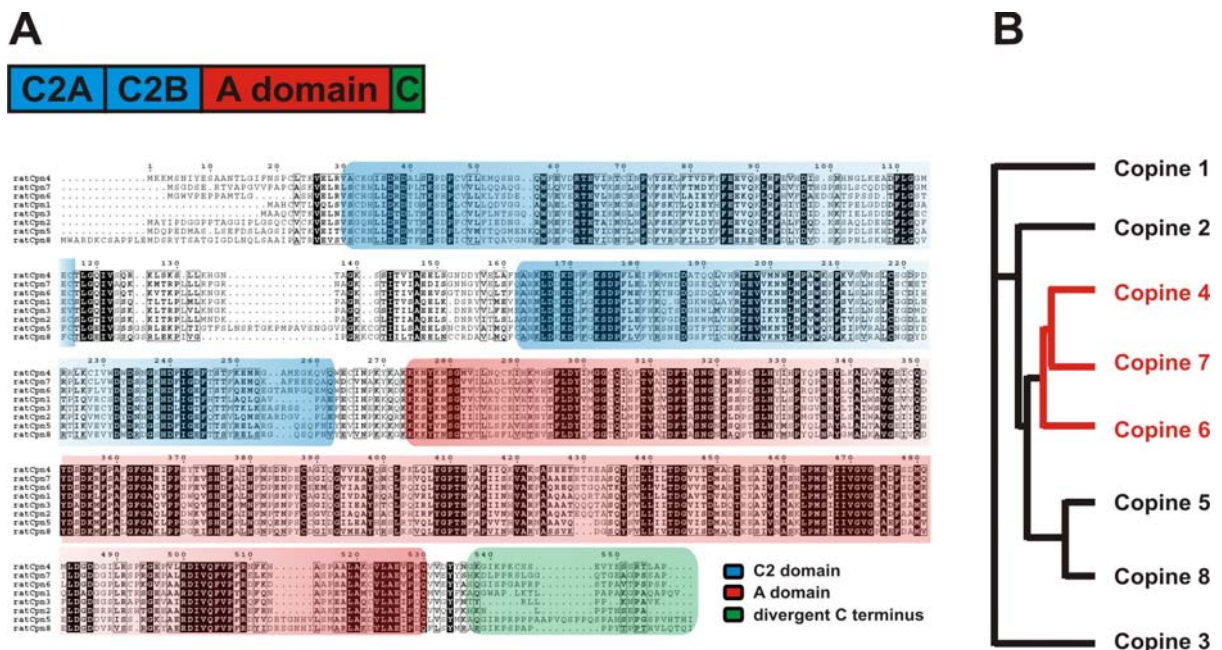


**Figure 9: The Copine family; structure and similarity**

(A) Overall structure of the Copine protein is determined by two calcium binding C2 domains (blue) at the N-terminus followed by an integrin-like A domain (red) and a highly divergent C-terminus (green). Sequences were aligned using ClustalW from the EMBL-EBI homepage. Residues of high homology are highlighted in black boxes. (B) Cladogram showing the relative copine homologies between the individual family members. Note that CNS specific copines (Cpne 4, 6 and 7 highlighted in red) share highest homology.

In different configurations (and at the C and not the N-terminus) these domains are also found in other calcium-sensing proteins like synaptotagmin [55], protein kinase C (PKC), phospholipase C (PLC) and Doc2 [56]. Like for PKC it was shown for Copine 1 that its interaction is mainly restricted to negatively charged phospholipids, like phosphatidylserine. Phosphatidylcholine or other neutral phospholipids are not or only very weakly bound by

---

Copine 1 [57]. This indicates a very interesting Copine characteristic; the preference for certain membrane compositions. Interestingly, despite their conserved amino acid sequence and architecture, not all Copines are expressed in all tissues e.g. Copine 4, 5 and 6, which show the highest similarity of all Copines (**Fig. 9B**), are found exclusively in the brain. The rest of the Copine family members are ubiquitously expressed [58]. Furthermore, the elevation of calcium also induces a Copine-Copine interaction which can be either of homo- or heteromeric kind [57]. The different domains of Copine proteins, especially the A domain, were the focus of a study performing a yeast two hybrid approach using the A domain of Copine 1, 2 and 4 as a bait to further elucidate its presumptive protein-protein interaction capability based on the formation of a characteristic coiled-coiled structure [59]. The fact that the A domains derived from different Copine isoforms bind to different target proteins including MEK1, protein phosphatase 5 (Copine 1 and 2) and Cdc42-regulated kinase (only Copine 4) provides evidence that Copines are members of an universal calcium-dependent transduction pathway [59]. In comparison to other studies which completely neglect the role of Copines in development, Copine 1 was identified in a proteomic screen from mouse brain covering the time of neural tube closure (E8.5 – E10.5) [60]. Additionally Copine 5 was shown to be upregulated during embryonic stages E13.5-15.5 in certain brain areas, like ventricle III, ventricle IV and the lateral ventricle, but not in the fully developed adult mouse brain [61]. Further analysis on the protein level revealed that Copine 5 is also expressed in the hippocampus, ganglionic eminence and dorsal tectum [61]. Considering their expression pattern and the fact that in murine spleen only approximately 5% of all calcium sensors are of Copine origin [57], Copines might cover a multitude of physiological functions governed by a tightly controlled system taking advantage of small differences between the Copine isoform.

### **Copine 6 what is known so far**

Copine 6 formerly described as N-Copine (neuronal) was first isolated in a hippocampus based cDNA screening set up, taking advantage of Kainate injected mice (resulting in high neuronal activity) [62]. It was shown that the expression of Copine 6 correlates with the activity of neuronal networks, as *in situ* hybridization revealed the highest signals in high frequency-stimulated CA1 areas of hippocampal slices. Interestingly, Copine 6 expression was not only limited to brain areas with high activity, but in a multi-tissue Northern blot it was shown that expression was limited to the brain, with no expression in other organs at all [62]. Analysis of the Copine 6 protein content of brain samples taken at different developmental stages, revealed that Copine 6 is expressed postnatally. In a more detailed study, it was shown by immuno-histochemistry that Copine 6 expression is limited to the olfactory bulb and hippocampus. On the contrary low or no signal, was detected in cortical areas, the hypothalamus, the cerebellum and the brain stem [63]. Furthermore an intrinsic, mainly

---

through the C2B domain, mediated calcium dependent membrane interaction was described [63]. Finally, considering the fact that Copine 6 expression is localized and limited to brain areas of high synaptic plasticity, during postnatal periods. That neuronal activity, especially LTP protocols triggers this expression, and moreover the fact that Copine 6 itself possesses the capability to sense calcium and therefore react on changes in neuronal activity points to a pivotal role of Copine 6 in synaptic plasticity and probably a function in learning and memory.

---

# **Copine 6, a novel calcium sensor translating synaptic activity into spine plasticity**

Milos Galic<sup>1,4,5</sup>, Alexander Kriz<sup>1,5</sup>, Judith Reinhard<sup>1</sup>, Martijn Dekkers<sup>1</sup>, Réjan Vigot<sup>2</sup>, Yan-Ping Zhang<sup>3</sup>, Gabriela Bezakova<sup>1</sup>, Bernhard Bettler<sup>2</sup>, Thomas G. Oertner<sup>3</sup>, Markus A. Ruegg<sup>1</sup>

<sup>1</sup>Department of Neurobiology and Pharmacology, Biozentrum, University of Basel, Klingelbergstrasse 70, 4056 Basel, Switzerland

<sup>2</sup>Department of Clinical-Biological Sciences, Institute of Physiology, Pharmazentrum, University of Basel, 4056 Basel, Switzerland

<sup>3</sup>Friedrich Miescher Institute, 4058 Basel, Switzerland

<sup>4</sup>Current address: Department of Chemical and Systems Biology, Stanford School of Medicine, USA

<sup>5</sup>These authors contributed equally

---

## **Summary (manuscript)**

Changes in synaptic activity alter synaptic transmission, ultimately changing neuronal network dynamics. Importantly, shifting synaptic properties often induces calcium-dependent structural rearrangements. The consequence of activity-dependent influx of calcium has been well studied and many of its targets have emerged over the last years. However, most of these studies are emphasizing the interaction of these proteins but ignore mechanisms controlling its spatio-temporal properties. Here we introduce a novel mechanism for activity dependent synapse plasticity based on protein translocation. We were able to demonstrate increased synaptic activity upon loss of Copine 6 in hippocampal neurons and show its enrichment in postsynaptic compartments upon NMDA receptor dependent calcium influx. Moreover, we show evidence for Copine 6 acting as a shuttle protein for the small Rho-like GTPase Rac1. In the presence of Copine 6, Rac1 shows calcium dependent enrichment at cell membranes. Interestingly neurons expressing a calcium-insensitive version of Copine 6 lose active synapses. Together, this provides evidence that Copine 6 translates synaptic activity into morphological changes through translocation of Rac1 into synaptic structures in a calcium-dependent manner.

---

## Introduction (manuscript)

Spines are the principal postsynaptic sites of excitatory synapses and may function as the basic unit of synaptic integration [11, 64]. Formation of spines is established by sequential cellular events [65, 66] and is accompanied by the transformation of dendritic protrusions into mature spines [12, 13]. Even after their establishment, spines are still motile and change shape and size [67-69]. In adult brain, activity-dependent changes in spine structure and number are thought to provide neural circuits with the ability to rewire and which could contribute to learning and memory [70-72]. Several molecules have been identified as potential regulators of spine morphology. Analysis of its function showed regulation at distinct levels. Some of the molecules, regulate position and quantity of individual proteins through relocalization [73-75], transcription [76-78] and degradation [79, 80]. While, a second group composed of kinases and phosphatases appears to be required for the regulation of these processes [81, 82], suggesting a hierarchical organization in spine formation and maturation. To induce the formation, elaboration or elimination of dendritic spines, many of these factors exert their effects by signaling to the actin cytoskeleton [83-85] and the function of these proteins is often regulated by activity-induced changes in the intracellular calcium concentration [86].

Copines are cytosolic proteins characterized by two C2 domains at the amino-terminus and an A domain at the carboxy-terminus (**Fig. 9A**). Eight Copines are predicted in mammals based on sequence identity and structural homology (**Fig. 9**). C2 domains are calcium and phospholipid-binding domains [57]. The A domain of Copines is capable of interacting with a wide variety of proteins that are themselves components of intracellular signaling pathways [59]. Several lines of evidence suggest that Copines are important for translocating their interacting partners to the immediate vicinity of plasma membranes upon calcium influx [53, 87]. In consequence, Copines affect the localization of target proteins. *In vivo* and *in vitro* studies have further shown that Copines are involved in a wide range of biological activities including exocytosis, gene transcription, phosphorylation, protein degradation, cytoskeletal organization and the targeting or stabilization of receptors at the plasma membrane [88, 89]. Most of the Copines are expressed ubiquitously, whereas Copine 6 expression is restricted to the brain. Moreover, Copine 6 expression in hippocampal neurons is upregulated upon kainate injection and after induction of long term potentiation (LTP) [62].

Here, we addressed the role of Copine 6 during synapse formation in cultured hippocampal neurons. We find that expression of Copine 6 is upregulated during synapse formation. Loss of Copine 6 increases the density of synapses while overexpression of native Copine 6 shows no effect. Intriguingly overexpression of a calcium-insensitive Copine 6 mutant causes the reduction of dendritic protrusions providing evidence for a calcium-dependent function.

---

We also show that these effects are likely to be caused by Copine-dependent regulation of the small Rho GTPases Rac1. Thus, our work is the first to describe a new role of Copines at synapses of the central nervous system.

## Results

### Timepoint of synapse formation in primary hippocampal neurons

To investigate whether expression of Copine 6 was upregulated during synaptogenesis between neurons, we first evaluated the timepoint of synapse formation and maturation in our primary hippocampal culture system. In accordance with previous reports we observed that nerve terminals establish contacts with postsynaptic structures between DIV7 and DIV11 but that the number of these contacts and incorporation of AMPA receptors at postsynaptic sites occurs at later stages, namely between DIV11 and DIV15 (**Fig. 10**).

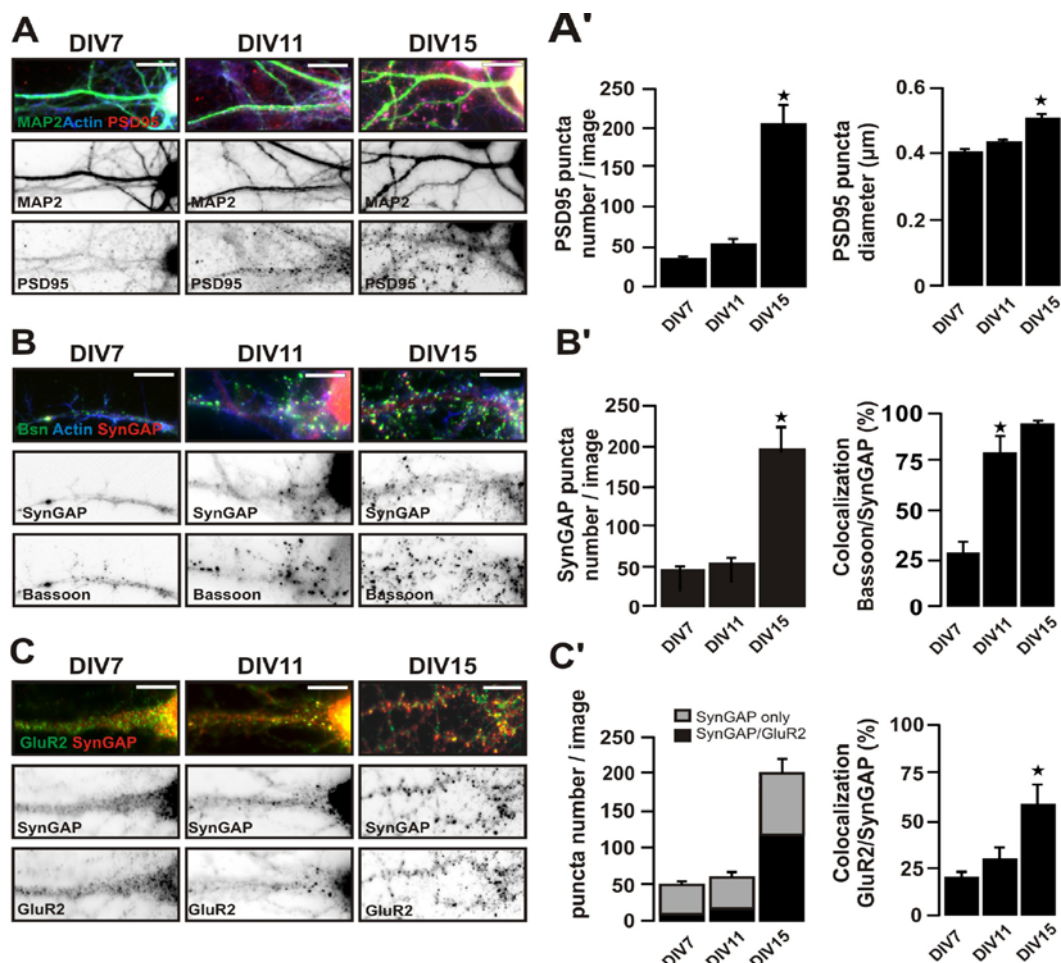


**Figure 10: Time course of synapse formation in primary hippocampal neurons**

(A) Primary hippocampal culture stained for actin (blue), the dendritic marker MAP2 (green) and the postsynaptic scaffolding protein PSD95 (red). Single channels depicting MAP2 and PSD95 staining are shown below. (A') Quantification of the number (left) and the diameter (right) of PSD95-positive puncta. A significant increase in the number and diameter of such puncta is observed between DIV11 and DIV15. (B) Neuron stained for actin (blue), the presynaptic marker Bassoon (Bsn, green) and the postsynaptic scaffolding protein SynGAP (red). Single channels depicting SynGAP and Bassoon staining are shown below. (B') Quantification of the number of SynGAP-positive puncta per picture (left) and the percentage of colocalization between Bassoon and SynGAP (right) is shown. Like PSD95-positive puncta (A', left), the number of SynGAP-positive puncta increases the most between DIV11 and DIV15. In contrast, co-localization of pre- and postsynaptic elements is essentially completed at DIV11. (C) Neuron stained for the AMPA receptor subunit GluR2 (green) and SynGAP (red). Single channels depicting SynGAP and GluR2 staining are shown below. (C') Quantification of the relative percentage of GluR2/SynGAP co-localization (right) and the number of GluR2- and SynGAP-positive puncta (left) is shown. Note that the number of puncta given represent the number per image and not per neuron because of the strong dendrite arborization at DIV15. For each image, regions were selected with similar neuron density and the puncta on the soma were not included. Data are derived from two independent experiments. For each parameter, 1520 pictures and more than 800 clusters were counted. Data represent mean  $\pm$  SEM. \* $p < 0.01$  compared to the previous time point. Scale bar = 10  $\mu$ m. Immunofluorescence in all the black and white pictures was inverted. (adapted from Galic & Kriz et. al)



---

## Copine 6 expression and location in the CNS.

We next monitored the expression of genes during this time window in primary hippocampal cultures. Gene expression was measured at DIV8, DIV10, DIV12 and DIV 14 by real-time RT-PCR and was normalized to the housekeeping gene 5-glyceraldehyde-3-phosphate dehydrogenase (GAPDH). For each gene, the first point of detection was arbitrarily set to 1. This initial screen identified Copine 6 to be upregulated (**Fig. 11A**). As shown in **Figure 11A'**, expression of another housekeeping gene, phosphoglycerolkinase 1 (PGK1), was not altered while expression of the postsynaptic protein SynGAP was highly increased during synapse formation. Next, we tested whether the upregulation could also be detected on the protein level. Indeed, expression of Copine 6 substantially increased in hippocampal cultures (**Fig. 11B**, left panel) and in lysates of rat cerebral cortex (**Fig. 11B**, right panel) at the peak of synaptogenesis. This expression data indicates a role for Copine 6 in processes in the already developed brain rather than in embryonic stages. To further analyse Copine 6 expression in different brain areas we dissected adult rat brains into olfactory bulb, frontal cortex, motoric cortex, hippocampus, hypothalamus, cerebellum and brainstem samples. These fractions were justified via immunoblotting to the same amount of  $\beta$ -actin and further probed with Copine 6 antibody. Interestingly fractions like the olfactory bulb and hippocampus known to be subjected to a steady rearrangement of neurons and synaptic plasticity show higher Copine 6 signals (**Fig 11C**, lane 1 and 4). Additionally staining of coronal sections of adult rat brains revealed that Copine 6 immunoreactivity was highest in the hippocampal CA3 area and dentate gyrus whereas only lower levels were observed in the cortex (**Fig. 11D**). Immunostaining directed against the dendritic marker MAP2 in cultured hippocampal neurons showed that Copine 6 localized to dendrites but not to axons (**Fig. 11E**). To further investigate the localization of Copine 6 within dendrites, we next transfected organotypic hippocampal slice cultures with a Copine 6-GFP fusion construct. To get a volume-independent measure of Copine 6 concentration in neurons we co-transfected the fusion protein with a freely diffusible red fluorescent protein (RFP). Copine 6-GFP fluorescence was always normalized to the RFP fluorescence. When we compared normalized signal intensities for Copine 6-GFP in dendritic spines to the signal found in the dendrites proper, we found that Copine 6-GFP was enriched by approximately 1.6-fold (**Fig. 11F**).

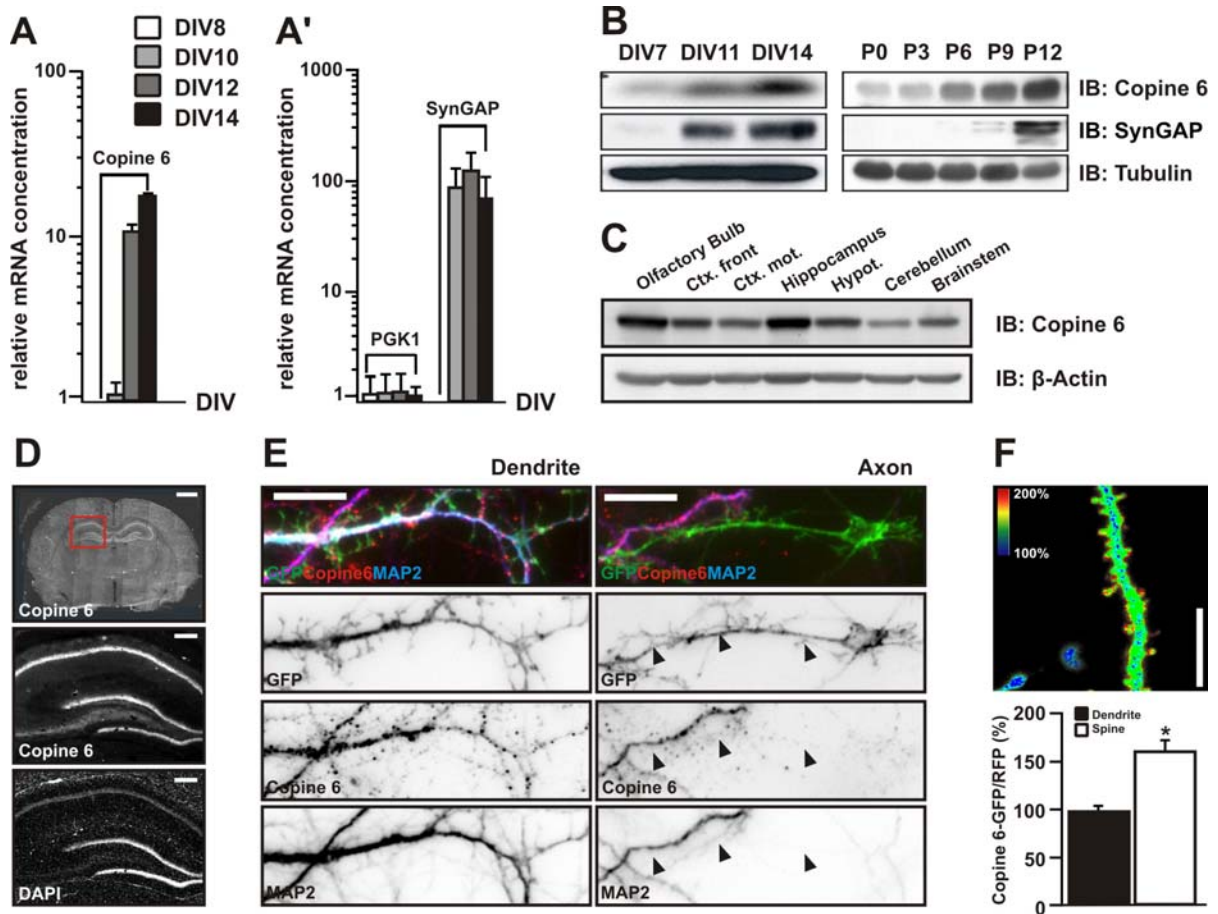


**Figure 11: Copine 6 expression and location in the CNS.**

(A) Expression levels of Copine 6 during synapse formation in primary hippocampal cultures as determined by quantitative real-time PCR. Values are plotted in a semi-logarithmic scale showing the relative mRNA concentration normalized to GAPDH (for primers see materials and methods). (A') Expression of the housekeeping gene, phosphoglycerolkinase 1 (PGK1), did not change during synapse formation, while expression of the synaptic protein SynGAP was upregulated. Note that SynGAP was normalized to GAPDH but not set arbitrarily to 1 at first appearance since expression at DIV10 was already 100-fold above detection level. Data represent mean  $\pm$  SEM from three independent experiments, each time point was analyzed in triplicates. (B) Left panel: Western blot analysis of Copine 6 (top) and SynGAP (middle) in primary hippocampal cultures at DIV7, DIV11 and DIV14. Tubulin was used as loading control (bottom). Right panel: Western blot analysis of rat cortex isolated at postnatal day 0, 3, 6, 9 and 12. Note, that Copine 6 is upregulated during the peak of synaptogenesis *in vitro* and *in vivo*. (C) Western blot analysis of different brain regions from adult rat. Samples were adjusted to the housekeeper  $\beta$ -actin and Copine 6 content was visualized with a Copine 6 antibody. (D) Coronal rat brain sections were probed with a Copine 6 antibody for their Copine 6 content. Scale bars are 1mm (top) and 200  $\mu$ m (middle and bottom) (E) Primary hippocampal cultures were transfected at DIV 7 with a synapsin driven GFP construct, fixed at DIV 12, and immunostained with Copine 6 antibody. MAP2 staining defines dendrites (left), while axons (right) are MAP2 negative but GFP positive. Scale bars = 10  $\mu$ m. (F) Picture of organotypic cultures from rat hippocampus transfected with GFP-tagged Copine 6 in conjunction with the freely diffusible tdimer2 RFP. Picture illustrate ratio of green (Copine 6-GFP)/red (tdimer2 RFP) fluorescence in rainbow colors. Blue and red represent the ratio indicated in each picture. Quantification of Copine 6-GFP concentration in spines after normalization to the values in dendrites is shown below. Data are mean  $\pm$  SEM (n = 40 spines in 5 cells). \* p < 0.01. Scale bar = 10  $\mu$ m.

---

## **Copine 6 binds reversibly to the Plasma Membrane in a calcium dependent manner**

We next focused on membrane binding properties of Copine 6. C2 domain containing proteins like PKC and Doc2 increase their affinity to certain phospholipids upon calcium elevation. In order to examine and analyze Copine 6 specific translocation kinetics we took advantage of a COS7 cell based assay. We were able to show that membrane fractions of COS7 cells prepared in the presence of calcium were enriched with Copine 6 whereas calcium-depletion via EDTA reverses the effect to a mainly cytosolic enrichment (**Fig. 12A** left). Treatment of COS7 cells with ionomycin, an ionophore increasing the membranes permeability for calcium shows that the majority of Copine 6-GFP signal changed from a homogenous cytoplasmic to a spotted membrane-bound one (**Fig. 12A** middle). Addition of EDTA to the COS7 medium prior to the ionomycine treatment abolished the clustering of Copine 6-GFP, clearly indicating that an increase in cytosolic calcium concentration was required (**Fig. 12A** right). To analyze the calcium concentration needed to induce membrane enrichment we incubated homogenates under various conditions and subsequently separated them into cytoplasmic and membrane fractions (**Fig. 12B** left). We were able to show that 5  $\mu\text{M}$  of calcium significantly increased the amount of Copine 6 bound to the membrane whereas 1  $\mu\text{M}$  had just a slight effect (**Fig. 12B'** top). To address the question if Copine 6 enrichment at the membrane is reversible, homogenates prepared in the presence of calcium were aliquoted and treated with different concentrations of EGTA (**Fig. 12B** right). Analyzing these fractions showed that membrane fractions which were treated with high EGTA levels showed a lower signal than untreated fractions demonstrating reversibility in Copine 6 plasma membrane binding (**Fig. 12B'** bottom).

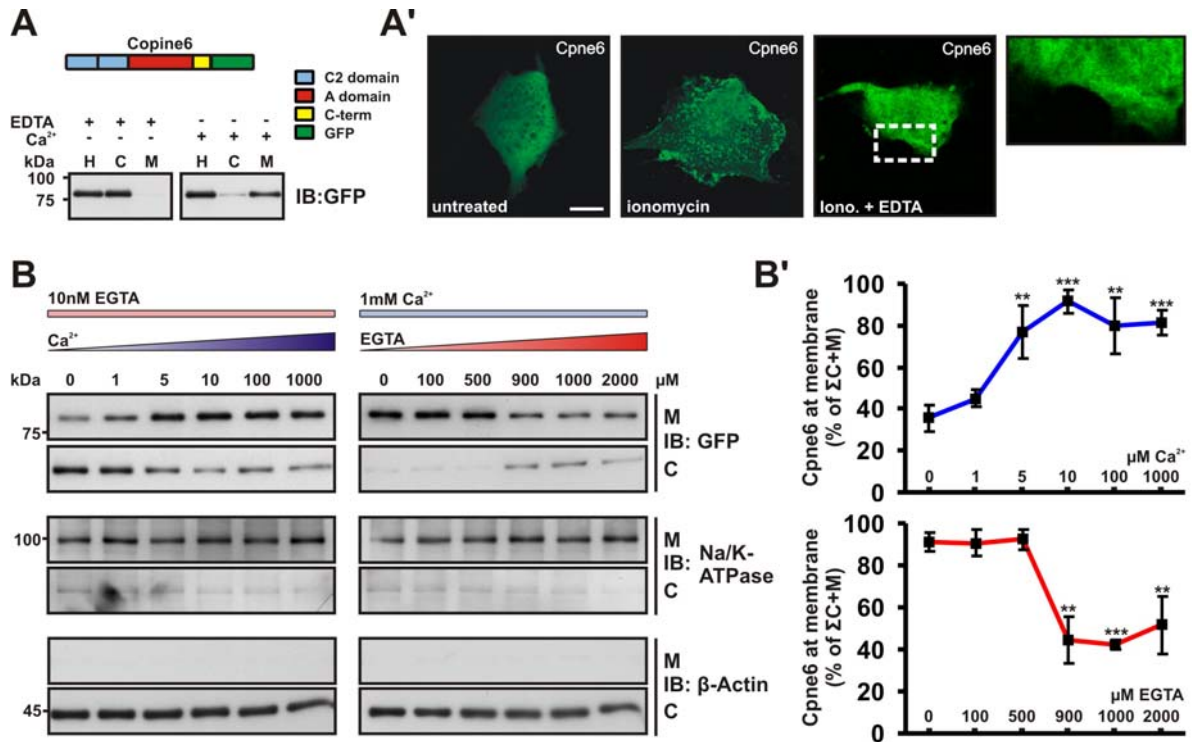


**Figure 12: Copine 6 binds reversibly to the plasma membrane in a calcium dependent manner**  
**(A left)** Homogenate fraction (H) derived from COS7 cells expressing Copine 6-GFP were fractionated into Membrane (M) and Cytoplasmic (C) in the presence (2 mM CaCl<sub>2</sub>) or absence (2 mM EDTA) of calcium. **(A')** Immunofluorescence of untreated COS7 cells transfected with Copine 6-GFP (left), after treatment with ionomycin (right) or ionomycin in the presence of EDTA. Scale bar = 20 μm. **(B)** Dosage effect of rising calcium or EGTA levels, respectively, on Copine 6-GFP localization to plasma membranes (M) or cytoplasm (C). **(B')** Copine 6-GFP localization to plasma membranes as a function of calcium or EGTA levels. The sum of the cytoplasmic and membrane fraction was considered as 100% and the ratio at the plasma membrane plotted. N=3 (calcium ramp) and N=3 (EGTA ramp); \* p < 0.05, \*\* p < 0.01, \*\*\* p < 0.001.

### Copine 6 affinity to plasma membranes is strengthened by cholesterol rich domains

Since the Copine 6-GFP membrane staining was not observed as a homogenous enrichment we wondered if Copine 6 may bind to specific membrane areas. Staining for cholesterol rich domains showed that Copine 6-GFP colocalized with lipid raft markers like Cholera toxin B1 in ionomycin treated COS7 cells (**Fig. 13A**). Moreover, Copine 6 colocalized in a calcium-dependent manner with the lipid raft marker Flotillin-1 in rat brain derived detergent resistant floating fractions (**Fig. 13A'**). Lipid rafts or detergent resistant membranes are among others characterized by elevated cholesterol content. To investigate its role in Copine 6 binding to membranes, we applied cyclodextrin that depletes cholesterol from membranes and therefore destabilize lipid rafts. Pre-treating COS7 cells with 10 mM of cyclodextrin for 1 hour before fractionation significantly inhibited Copine 6 enrichment at membranes in the presence of calcium, conferring that Copine 6 affinity to membranes depends on cholesterol rich structures like lipid rafts (**Fig. 13B and B'**).

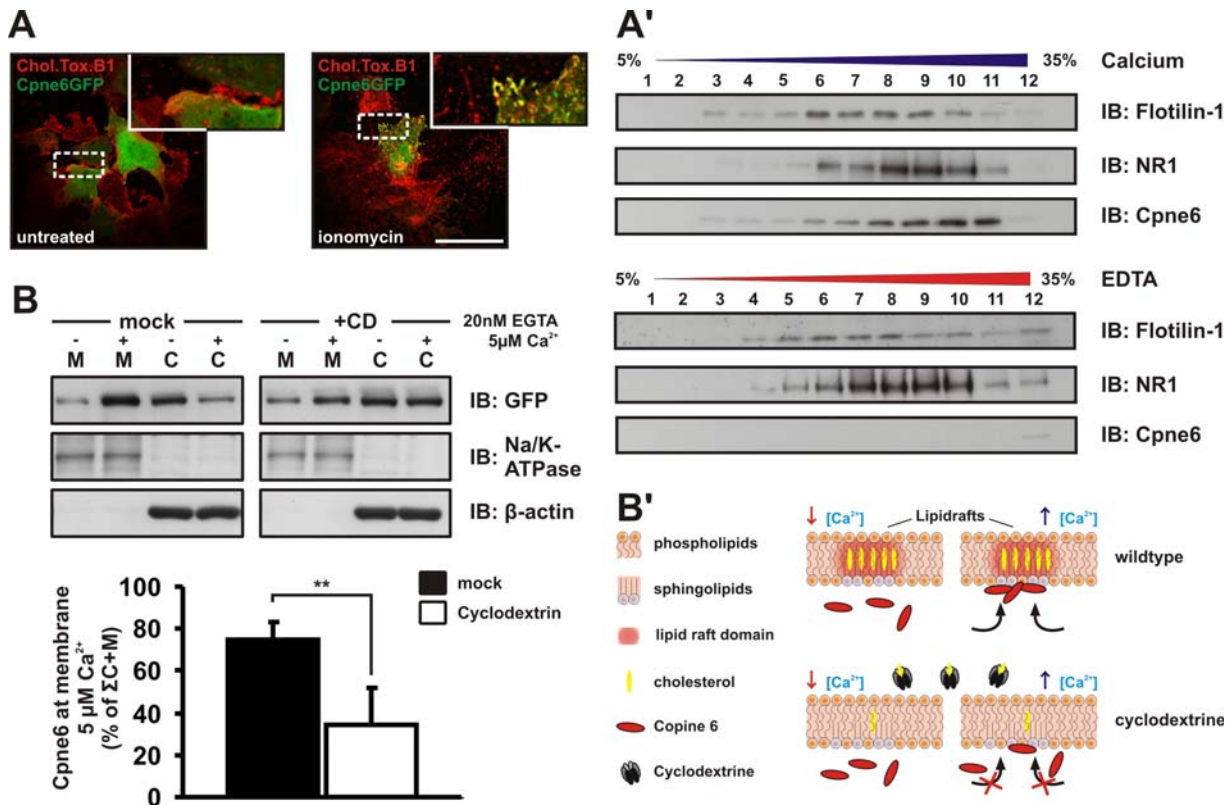


**Figure 13: Copine 6 affinity to plasma membranes is strengthened by cholesterol rich domains**

(A) Cholera toxin B1 stained lipid rafts of COS7 cells transfected with Copine 6-GFP in the presence (right) and absence (left) of ionomycin. Scale bar = 50  $\mu\text{m}$ . (A') Detergent resistant lipid raft enriched floating fractions derived from adult rat brains upon treatment of changing calcium and EDTA conditions. 2.5  $\mu\text{g}$  of total protein was loaded for each fraction. Flotillin1, Copine 6 and the NMDAR subunit NR1 were detected by immunoblotting. (B) COS7 cells expressing Copine 6-GFP incubated with or without cyclodextrin resulting in an either unchanged or depleted cholesterol content followed by membrane (M) and cytoplasm (C) fractionations. Quantification of Copine 6-GFP signal in membrane fractions upon changed cholesterol content in the presence of calcium. Data represent mean  $\pm$  STDV from N=3; \*\* p<0.01. (B') The enrichment of Copine 6 at plasma membranes depends on lipid rafts stabilized by cholesterol.

### Ca<sup>2+</sup> dependent enrichment of Copine 6 in PSDs.

Immunoblotting of postsynaptic densities (PSD) derived from subcellular fractionations of adult rat brain in the presence of calcium show high reactivity with a Copine 6 antibody (Fig. 14A). Consistent with our previous findings, removal of calcium by adding EDTA during the fractionation process abolished the Copine 6 signal in PSD fractions and caused an increase in cytoplasmic fractions (Fig. 14A'). Interestingly the lipid raft marker Flotillin-1 was highly enriched in postsynaptic densities (Fig. 14A), indicating that synaptic membranes and in particular spine membranes represent hot spots for Copine 6 binding. Intriguingly, this explains Copine 6 enrichment in spines described above but more importantly implies calcium-induced translocation of Copine 6 from the cytoplasm into spines. In spines, the main source for elevated cytosolic calcium levels is calcium influx induced by synaptic activity, mainly through the NMDA-receptor and VDCC channels. We next studied the distribution of Copine 6 in primary hippocampal neurons in the presence of NMDA receptor and VDCC inhibitors (Fig. 14B). While Copine 6 translocation occurred in neurons treated with glutamate in the absence of NMDA antagonist APV, pre incubation of hippocampal



cultures with APV for 15min abolished the Copine 6 response. Furthermore, addition of trans-ACBD - a highly specific NMDA receptor agonist - triggered Copine 6 translocation. On the other side, blocking voltage dependent calcium channels (VDCC's) by pre incubation of neuronal cultures with Cadmium for 15min was not sufficient to block the glutamate triggered response (**Fig. 14B**). These data clearly identified the NMDA receptor as the main calcium entry point for Copine 6 translocation, providing evidence that synaptic activity translates into Copine 6 translocation.

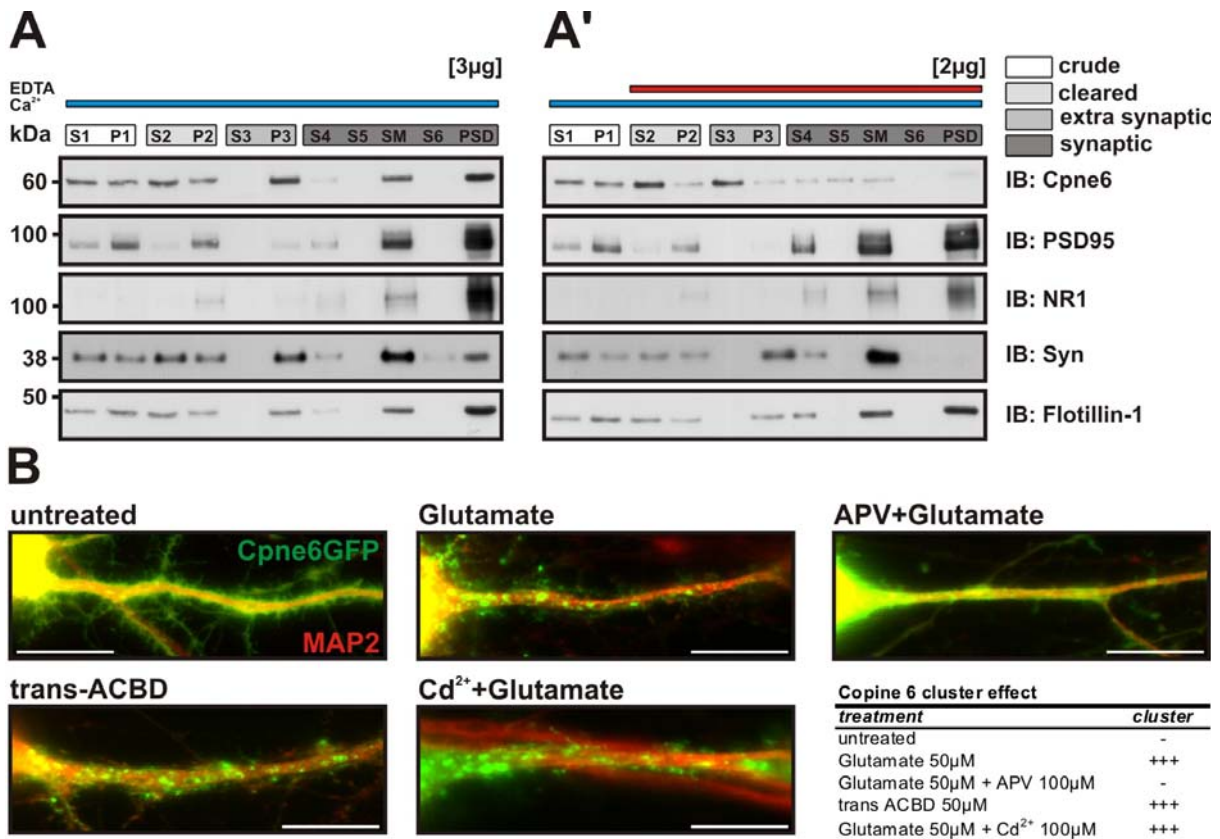


**Figure 14: Ca<sup>2+</sup> dependent enrichment of Copine 6 in PSDs.**

Subcellular fractionation of adult rat brain in the presence of calcium (**A**) and with EDTA added during the process (**A'**). Isolated fractions are, from left to right: post nuclear supernatant (S1); nuclear pellet (P1); crude cytoplasm (S2); synaptosomal-mitochondrial pellet (P2); cytoplasmic proteins (S3); microsomal and plasma membranes (P3); post synaptosomal supernatant (S4); synaptosomal cytoplasm (S5); synaptic membranes (SM); post postsynaptic density supernatant (S6); postsynaptic densities (PSD). An equal amount of protein 3 µg (**A**) and 2 µg (**A'**) was subjected to immunoblotting for different synaptic and lipid raft markers as well as Copine 6. Copine 6 localization changes in a calcium-dependent manner. (**B**) DIV 12 hippocampal neurons expressing synapsin driven Copine 6-GFP were treated with the indicated pharmacological agents. Clustering of Copine 6 occurred after application of Glutamate and trans ACBD. Note, that addition of APV blocked Copine 6 translocation upon Glutamate application. Scale bar =20 µm.

### NMDAR mediated Copine 6 translocation

To monitor the spatio-temporal dynamics of Copine 6 distribution more closely, we transfected hippocampal neurons with a cytosolic tdRFP construct together with a Copine 6-GFP fusion protein. At DIV 14 neurons were treated with 10 µM of NMDA triggering opening of synaptic NMDA receptors. As indicated in **Figure 15A**, NMDA application induced translocation of Copine 6 within 4 minutes after induction. This translocation is visualized as

a depletion of Copine 6 in the cytoplasm of the dendritic shaft (increase in red signal) together with a subsequent green outlining of the neuron. Moreover, high magnification microscopy showed that the translocation causes an increase of Copine 6 in post synaptic structures (**Figure 15A** inset, **Movie S1, S2** and **S3**). Dividing the Copine 6-GFP signal intensity of single spines after the NMDA application with the initial intensity of the basal state, we were able to estimate that Copine 6-GFP enriched in spines about 4 times upon NMDA application (**Fig. 15B**). Since the NMDA receptor plays a pivotal role in synaptic plasticity it raised the question which function Copine 6 translocation may have. To probe for a functional role of Copine 6 in synapse formation we decided to perform RNA interference experiments.

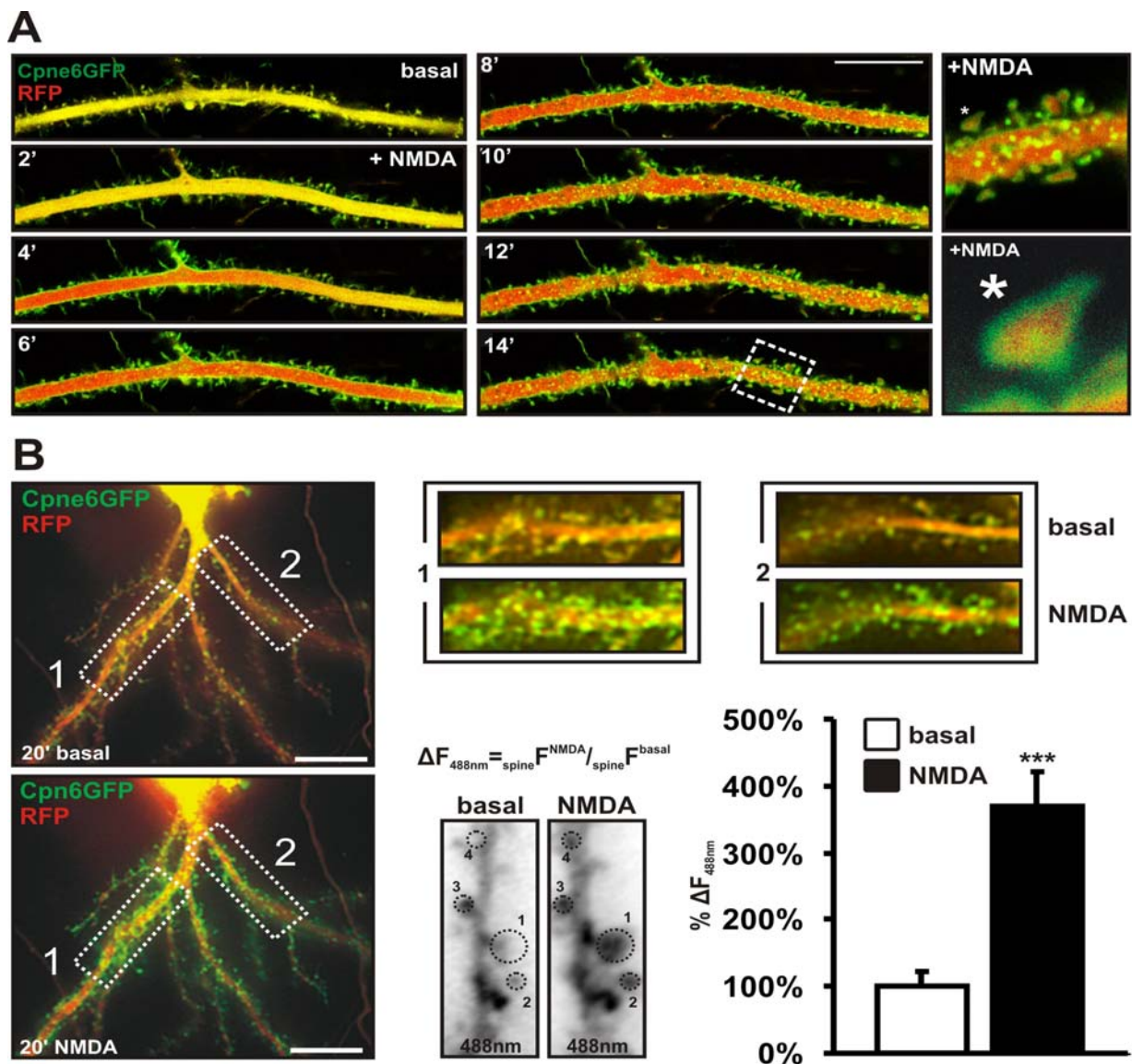


**Figure 15: NMDAR mediated Copine 6 translocation**

(**A**) Kinetics of Copine 6 translocation was visualized by DIV 14 hippocampal neurons expressing Copine 6-GFP together with cytosolic tdRFP. A dendritic stack picture is shown covering pre NMDA application time (basal) until 14 minutes post NMDA application. The dendrite at 14 min post NMDA application is blown up for better visualization (insets to the right). (**B**) Quantification of Copine 6-GFP enrichment at spines upon NMDA application. Representative dendritic stretches (1 and 2) were amplified for better visualization of Copine 6 enrichment (right). Analysis: the 488nm signal was converted in a grey value and pixel intensities of spine areas were quantified. The intensity measured in the basal state was set to 100%. The graph depicts average of 70 spines from 4 dendritic stretches of 2 cells. Mean values are shown, with +/- SEM, \*\*\*  $p < 0.001$ . Scale bar = 20  $\mu m$ .

We identified two 21 bp-long shRNA sequences that were cloned into a vector driving RNA expression under the U6 promoter (materials and methods for sequences). The shRNA constructs were then tested in COS cells for their capability of suppressing expression of a co-transfected Copine 6-GFP fusion protein (**Fig 16A**). In primary hippocampal cultures, all experiments were performed with both shRNA construct, but quantified for the more potent. Cultured neurons were co-transfected at DIV7 with a green fluorescent protein (GFP) expression vector in combination with shRNA to Copine 6 or to CD4 (as control). When we examined 5 days later (i.e. DIV12) the overall morphology of transfected neurons, knockdown of Copine 6 caused dendrite ruffling. Co-expression with RFP-tagged  $\beta$ -actin showed that the ruffling is the consequence of a discontinuous outgrowth of actin-positive protrusions along the dendritic shaft (**Fig. 16B**). Interestingly the amount of globular actin enriched structures which were considered as spines were increased while the density of filopodia was unchanged in the Copine 6 knock down. We next asked if these observed globular structures may represent synapses.

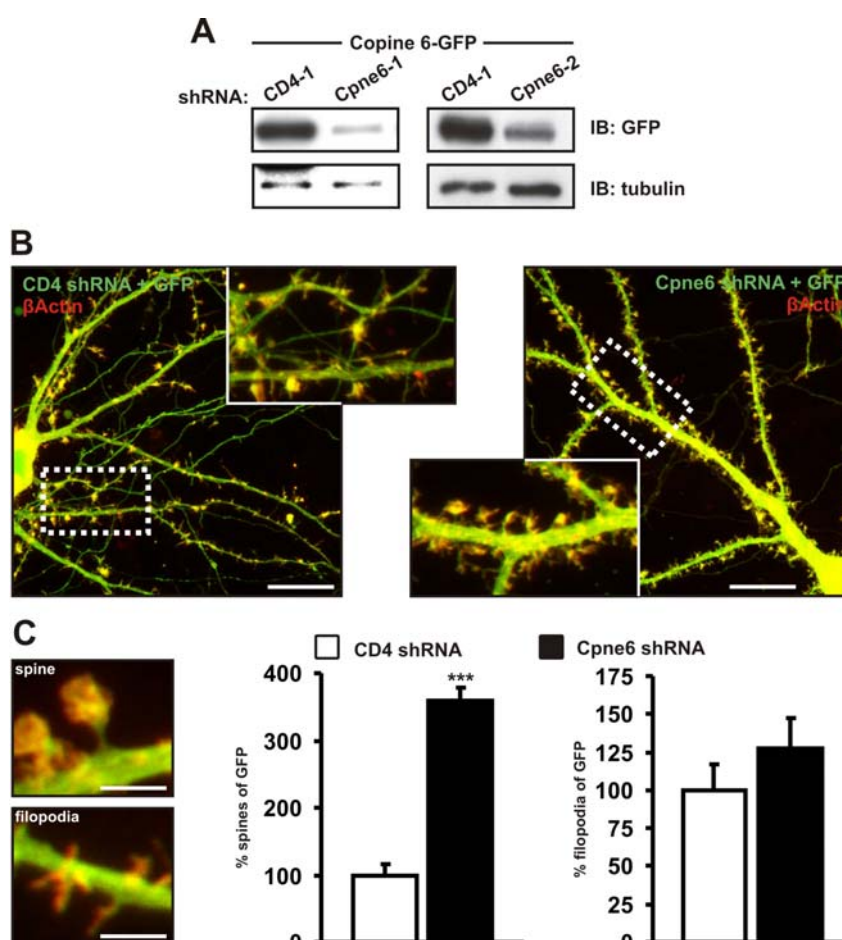


**Figure 16: Loss of Copine 6 increases  $\beta$ -actin positive protrusion density**

(**A**) Testing of both shRNA constructs to Copine 6. (**B**) Representative pictures of DIV 14 primary hippocampal neurons co transfected with either shRNA to CD4 or shRNA to Copine 6 together with  $\beta$ -actin-tdRFP. Scale bar = 20  $\mu$ m. (**C**) Quantification of  $\beta$ -actin-tdRFP positive protrusions classified as either spines or filopodia depending on their morphology. Data is mean value  $\pm$  SEM per 10  $\mu$ m dendrite length N = 3 experiments with more than 12 neurons examined for each condition, \*\*\* $p < 0.001$ . Scale bar = 4  $\mu$ m.



---

### Loss of Copine 6 increases synaptic density

Quantification of PSD95-positive puncta showed that knockdown of Copine 6 caused a significant increase in the density and a slight, but not significant increase in the diameter of PSD95-positive puncta when compared to neurons transfected with shRNA to CD4 (**Fig. 17A and A'**). Importantly, co-expression of shRNA directed against Copine 6 together with an insensitive overexpression version of Copine 6 reversed both, the observed increase in PSD95 puncta as well as the endogenous Copine 6 levels. This is clearly showing that the observed effect was due to loss of Copine 6 (**Fig. 17B and B'**). Co-localization of postsynapses with presynaptic nerve terminals was quantified by measuring co-localization of SynGAP and Bassoon. Like for PSD95-positive puncta, the density of synapses (i.e. SynGAP and Bassoon-positive structures) was increased upon loss of Copine 6 (**Fig. 17C and C' left panel**). Moreover, the diameter of the synapses was not increased (**Fig. 17C', right panel**). To investigate whether these synapses were also functional, we measured miniature excitatory postsynaptic currents (mEPSCs) by whole-cell patch-clamp recording in DIV12 neurons. As shown in **Figure 17D and D'**, the frequency was significantly increased in neurons expressing shRNA to Copine 6 compared to control neurons, while the amplitude of the mEPSCs remained unchanged. To further proof electrophysiological data with morphological read out, we quantified the postsynaptic localization of the AMPA receptor which is crucial for synaptic activity (**Fig. 17D**). We find that 40% of all SynGAP-positive puncta also stained the AMPA receptor subunit GluR2 in neurons expressing shRNA to Copine 6. In contrast, only 20% of all SynGAP-positive puncta co-localized with GluR2 in control neurons lacking CD4 (**Fig. 17D', left panel**). Interestingly, the diameter of GluR2/SynGAP-positive synapses did not differ between neurons expressing shRNA to Copine 6 or CD4 (**Fig. 17D', right panel**). Thus, the overall increase in the density of SynGAP-positive structures (**Fig. 17C', left panel**) is based on an increase in the percentage of active, GluR2-containing synapses. In conclusion, knockdown of Copine 6 results in more functional synapses without changing their basic properties. These data suggests that Copine 6 itself may act as an inhibitor of synapse formation and/or maturation.

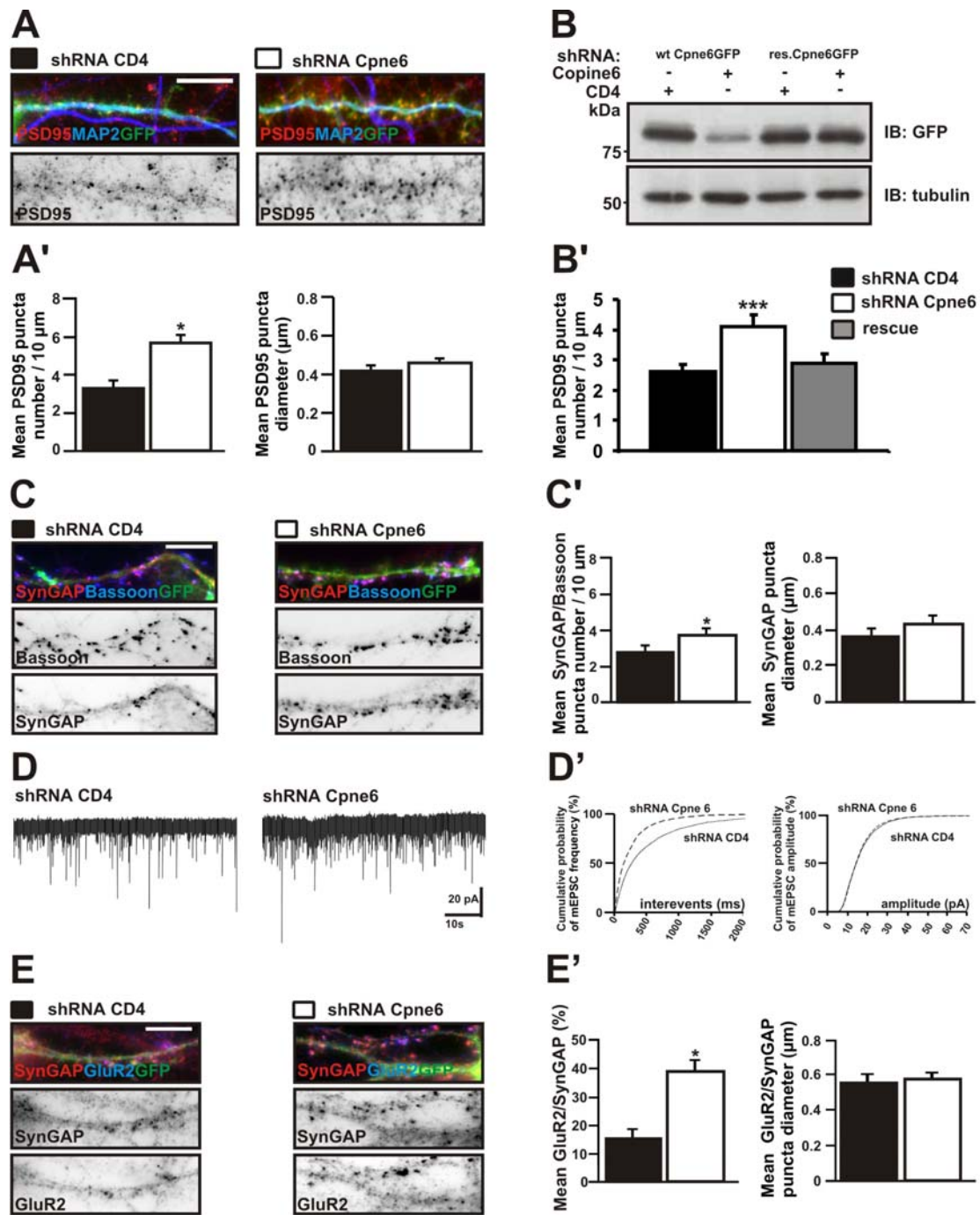


**Figure 17: Loss of Copine 6 increases synaptic density**

Analysis of cultured, primary hippocampal neurons at DIV12, 5 days after transfection with plasmids encoding GFP (green) and shRNA to CD4 (shRNA CD4) or Copine 6 (shRNA Copine 6). **(A)** Postsynaptic structures on dendrites (MAP2-positive, blue) were visualized with antibodies against PSD95 (red). **(A')** Quantification of the effect of shRNA to Copine 6 on the number of PSD95-positive structures in a segment of 10 μm (i.e. density) and their diameter. **(B and B')** Overexpression of a shRNA resistant Copine 6 mutant rescues the knock down effect. N=2 mean value in PSD95 puncta / 10μm shown +/- SEM. **(C)** Neurons stained for SynGAP (red) and Bassoon (blue). **(C')** Knockdown of Copine 6 results in an increase in the density of synapses stained for both Bassoon and SynGAP. Note that the density of SynGAP/Bassoon-positive structures is lower than that of PSD95-positive puncta. **(D)** Analysis of miniature excitatory postsynaptic currents (mEPSCs). Characteristic traces of transfected neurons are shown to the left. Knockdown of Copine 6 significantly increases the frequency but not the amplitude of mEPSCs **(D')** ( $p < 0.01$ , Kolmogorov-Smirnov test,  $n = 6$  neurons per condition, 800 events measured per neuron). **(E)** Expression of SynGAP (red) and GluR2 (blue). **(E')** Neurons expressing shRNA to Copine 6 have significantly more synapses containing both SynGAP and GluR2. In contrast, the diameter of GluR2-positive synapses shows no significant difference between Copine 6 knockdown and control spines. Note that GluR2/SynGAP-positive puncta are larger than postsynaptic SynGAP-positive structures. Data represent mean  $\pm$  SEM from two experiments,  $n = 20-25$  neurons per group,  $\geq 1000$  clusters per group. \*  $p < 0.01$ , \*\*  $p < 0.05$ . Scale bar = 10 μm.

## Overexpression of Copine 6 has no effect on neuronal morphology or synaptic transmission

We then asked what effect overexpression of Copine 6 may have. We examined hippocampal neurons at DIV 14 expressing Copine 6-GFP under a synapsin promoter driven plasmid for 7 days. To better visualize spine structures we co-transfected Copine 6-GFP with  $\beta$ -actin-tdRFP as actin is highly enriched in postsynaptic structures. To our surprise, our experiments showed no changes in the overall morphology of Copine 6-GFP expressing neurons compared to control neurons (**Fig. 18A**). Neither spines (globular heads positive for actin with neck like structures) nor filopodia (absence of globular structures, thin hair like actin positive fibers) did reveal any significant changes (**Fig. 18A'**). Finally, spontaneous transmission probability of Copine 6-GFP overexpressing neurons was measured by miniature Excitatory Postsynaptic Current recordings (mEPSCs). Like the previous parameters, mEPSC did not reveal significant changes in frequency or amplitude (**Fig. 18B and B'**). Together, this clearly shows that overexpression of Copine 6 has no effect on overall morphology, protrusion density or basic synaptic properties. In conclusion, this provides evidence that Copine 6 has no endogenous enzymatic activity. However, since other Copine family members were shown to both, bind to other proteins and translocate in a calcium-dependent manner, we speculated that Copine 6 may act as a calcium-dependent shuttle protein. According with such a role, overexpression of Copine 6 should not affect translocation of such a regulatory protein and in consequence not change synaptic properties.

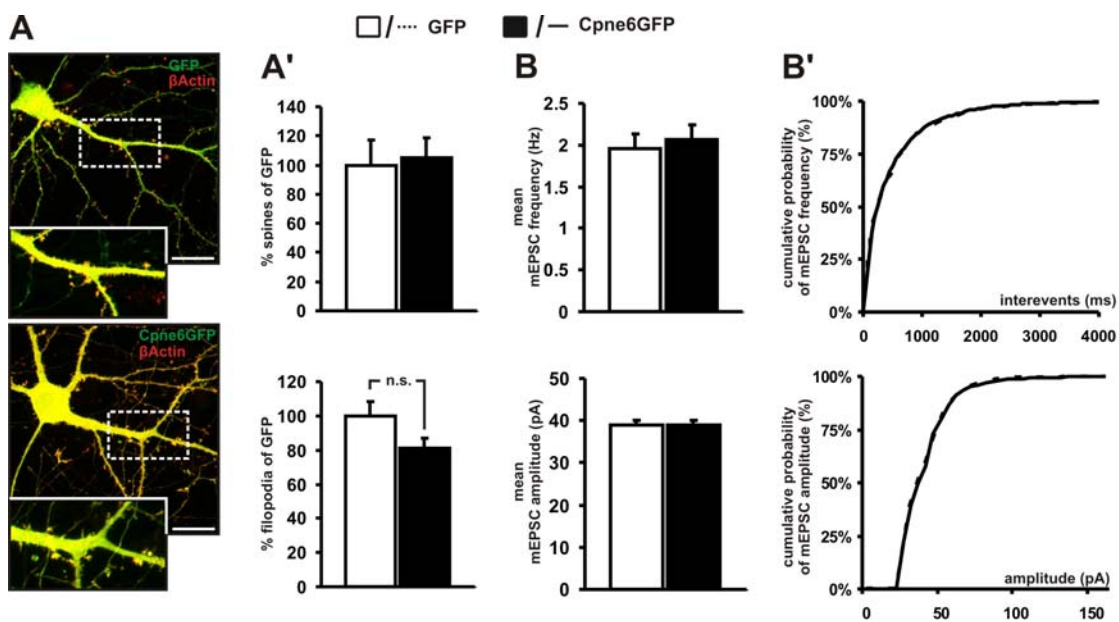


**Figure 18: Overexpression of Copine 6 has no effect on neuronal morphology or synaptic transmission**

(A) DIV 14 hippocampal neurons expressing  $\beta$ -actin-tdRFP together with empty synapsin driven GFP or Copine 6-GFP. (A') Quantification of spine (top) and filopodia (bottom) number of 10  $\mu$ m dendrite stretches normalized to the control (GFP). Mean values are shown,  $n=3$  more than 12 neurons for each condition  $\pm$  SEM. (B) Analysis of miniature excitatory postsynaptic currents (mEPSCs) show no changes in frequency (top) and amplitude (bottom). (B') No significant changes are visible in the cumulative plot. Kolmogorov-Smirnov test,  $n=9$  neurons per condition, more than 800 events measured per neuron. Scale bar = 20  $\mu$ m.

---

## **A calcium blind Copine 6 mutant causes spine loss and an increase in filopodia**

Analyzing the amino acid sequence of Copine 6 revealed a short stretch of amino acids in the C2B domain highly similar to so called EF-hand structures which also define the calcium binding motifs of PKC and synaptotagmin. Especially five aspartate residues were conserved in all proteins. In order to interfere with Copine 6 calcium interaction we substituted the aspartate residue at position 167 with an asparagine. The newly generated Copine 6D167N mutant was not able to be enriched at cellular membranes upon calcium influx in COS7 cells (**Fig. 19A, left and A'**), but stayed homogeneously distributed in the cytoplasm as shown with a GFP tagged mutant in an immunofluorescence approach (**Fig. 19A, right**). We then expressed Copine 6D167N in neurons. Like in COS7 cells Copine 6D167N location did not change in a calcium-dependent manner (**data not shown**). However, overexpression of the mutant led to a loss of dendritic spines and an increase in dendritic filopodia number (**Fig. 19B, bottom white arrows**). Importantly, the increase of filopodia occurred at the cost of spines since spine density significantly decreased (**Fig. 19B'**). The increase in filopodia (**Fig 19B'**) and concomitant loss of spines was accompanied by a tremendous decrease in mEPSC frequency (**Fig. 19C**). Analysis of mEPSC amplitude however points out that the properties of the remaining synapses were not changed (**Fig. 19C**). This proves our previous hypothesis that Copine 6 is required for the shuttling of a regulatory protein in a calcium or activity dependent manner. Our data further suggests, that knockdown of Copine 6 causes an increase of active synapses probably by freeing the otherwise to Copine 6 bound activator causing an unguided diffusion, completely naïve to neuronal activity. The same activator stays bound to Copine 6D167N in the cytoplasm subsequently depleting it from the synapse, thus simulating a synthetic low calcium, low activity level state causing the break down of synaptic structures into filopodia. We concluded that this activator must play a pivotal role in synaptic stability since its depletion causes the reformation of spines into filopodia. Considering the drastic change of the actin cytoskeleton in the knock down experiments, we speculated it may be an actin-reorganizing protein which by itself unable to respond to calcium changes or neuronal activity.

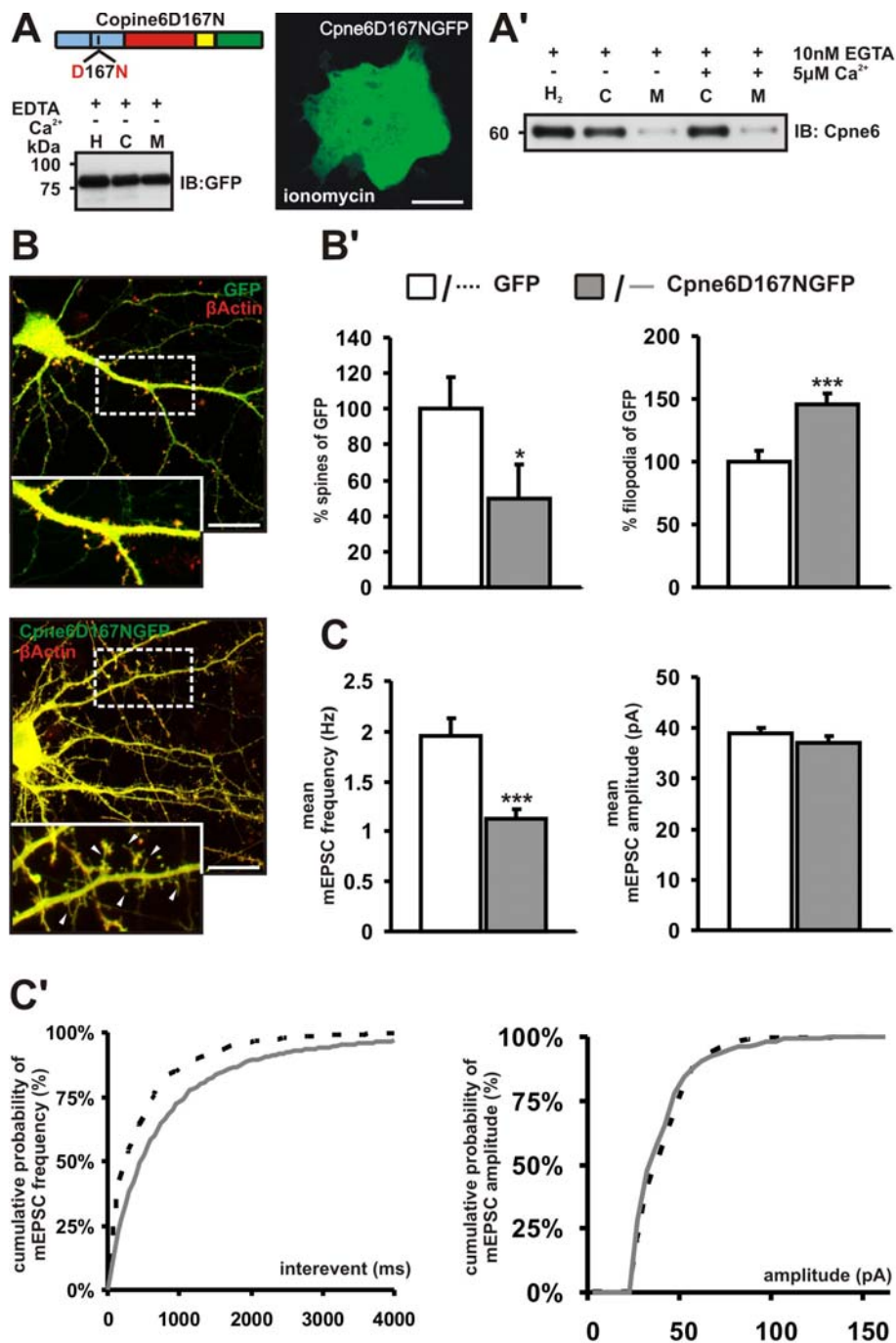


**Figure 19: A calcium blind Copine 6 mutant causes spine loss and an increase in filopodia**

Introducing a point mutation at position 167 causing a D to N transition into the Copine 6 C2B domain results in a “calcium blind” version of Copine 6 which lacks any calcium responsiveness (**A** and **A'**). (**B**) DIV 14 hippocampal neurons expressing an empty synapsin driven GFP or Copine 6D167N-GFP together with a β-actin-tdRFP. (**B'**) Quantification of spine and filopodia number at 10 μm stretches of dendrite shown as a density read out. Mean values are shown, n=3 more than 12 neurons for each condition +/- SEM. (**C** and **C'**) Analysis of miniature excitatory postsynaptic currents (mEPSCs) mean values are shown. Kolmogorov-Smirnov test, n= 9 neurons per condition, more than 800 events measured per neuron; \*\*\* p<0.001.

### Copine 6 recruits the small Rho like GTPase Rac1 to the membrane in a calcium dependent manner

We next aimed to identify this activator. The small GTPase Rac1 is known as one of the major developmental constituents in early phases of synaptogenesis. Recent studies directly link synaptic activity via CaMKII and certain GEF's like Kalirin 7 and Tiam 1 to changes in Rac1 activation levels in individual synaptic structures [90-92]. Moreover, changing the

---

activation level of Rac1 directly influences the stability of synapses. Due to this similarity in phenotypes, we hypothesized that Rac1 may be the activator we were looking for. If Rac1 is the principal target of Copine 6 and the effects shown upon loss of Copine 6 relied on a free, uncontrolled diffusion of Rac1 into synapses, inhibition of Rac1 should completely avert the Copine 6 shRNA effects. To prove this hypothesis, we applied NSC 23766, a Rac1 specific inhibitor which is blocking the Kalirin-7 and Tiam-1 GEF binding site of Rac1 but leaves other GTPases like Cdc42 and RhoA unaffected. **Figure 20A** shows that blocking Rac1 averted the increase of spine density upon loss of Copine 6, providing evidence that Rac1 is necessary in this process. Since the Rac1 inhibition had no effect on synapses in our control situation we assumed that fully matured synapses are not relying on activated Rac1 while the excess population in the Copine 6 knock down reflect a more unstable maybe not fully matured state of synaptic development. Moreover, the increase in filopodia density upon NSC 23766 application mimicked the effects upon overexpression of calcium insensitive Copine 6, indicating that local levels of Rac1 activity dictate both, spine maturation and degradation (**Fig. 20A'**). To check for direct interaction between Rac1 and Copine 6, we performed pulled down experiments. Both, wildtype and the calcium insensitive Copine mutant bound to a Rac1-GFP, indicating direct calcium independent interaction between the proteins (**Fig. 20B**). Next, we aimed to investigate if Copine 6 interaction was affected by the activity state of Rac1. This is not the case, as expression of Copine 6 together with the constitutive active, GTP-bound version of Rac1 (Rac1V12) or the dominant negative, GDP-locked form (Rac1N17) of Rac1 both showed co-immunoprecipitation (**Fig. 20B'**). We demonstrated so far that Copine 6 is responding to elevated calcium levels by translocating from the cytoplasm to the cell membrane as well as direct interaction with Rac1 suggesting that Copine 6 might influence the localization of Rac1 in a calcium dependent manner. To test this assumption, Copine 6-RFP and Rac1-GFP were transfected separately (**Fig. 20C**) or together (**Fig. 20C'**) into COS7 cells. Copine 6-RFP location changed drastically from a homogenous, cytoplasmic to a clustered, membrane stain upon ionomycin treatment. In contrast, Rac1-GFP signal remained cytoplasmic after ionomycin application (**Fig. 20C**). However, when Copine 6 and Rac1 were present in the same cell we observed Rac1 enrichment at the membrane in an ionomycin-dependent manner (**Fig. 20C'**). Importantly, this behaviour was not observed in Rac1 single transfected cells or cells which co express Cdc42 or RhoA together with Copine 6 (**Fig. 20C''**). Thus, we provide evidence for a Copine 6 dependent, calcium induced movement specifically for the small Rho-like GTPase Rac1 to the plasma membrane thus providing the GTPase with the ability to react upon calcium influx.



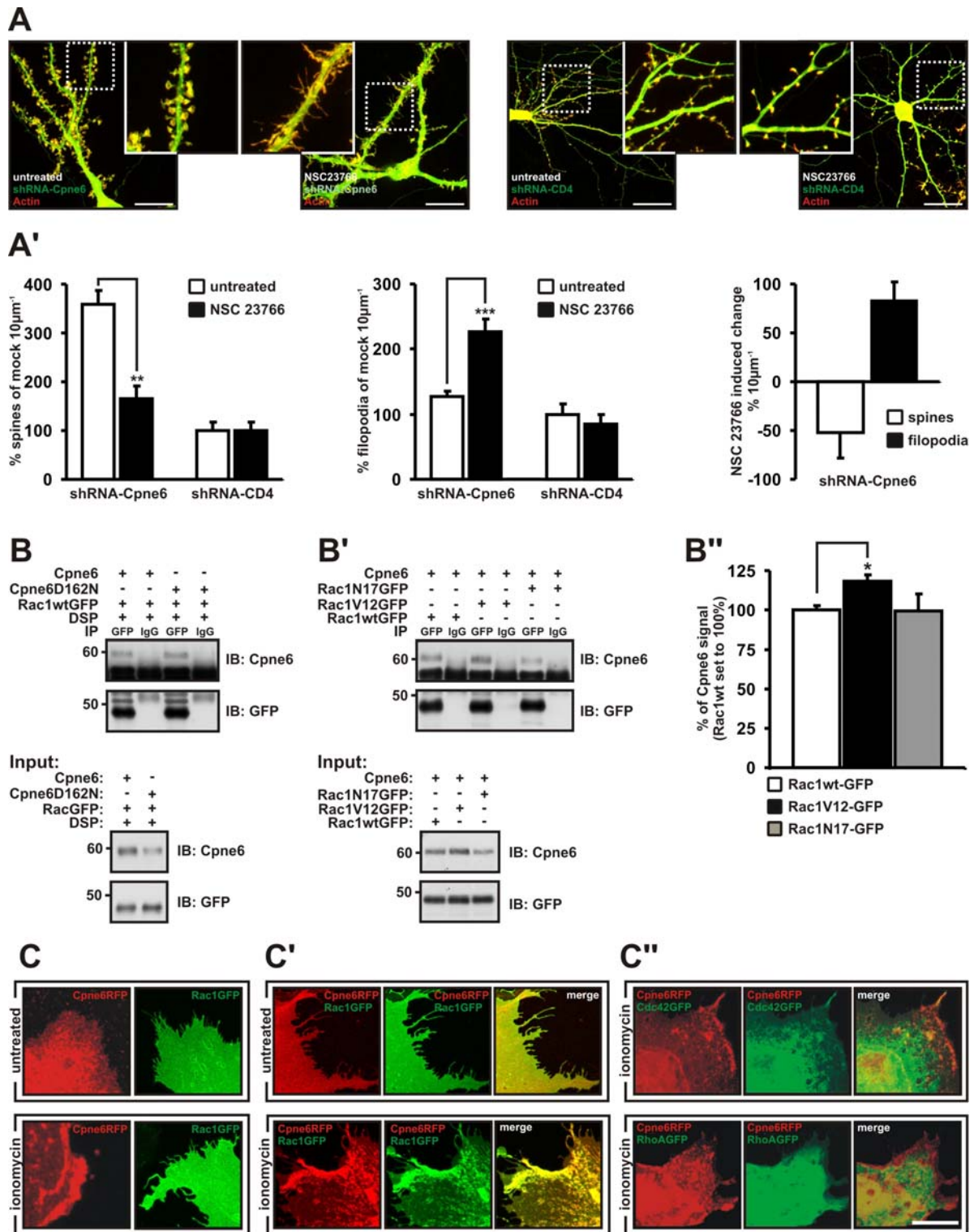


**Figure 20: Copine 6 recruits the small Rho like GTPase Rac1 to the membrane in a calcium dependent manner**  
 (A) DIV 14 hippocampal neurons transfected with the constructs indicated were either treated with the Rac1 inhibitor NSC 23766 or mock control o/n. The amount of spines (A' left) and filopodia (A' middle) per 10 μm of dendrite length were counted and quantified. The total change induced by NSC23766 is shown in A' right. Data shown is mean value +/- SEM from 12 neurons N=3 at least two dendrites per neuron were counted; \*\*\* p<0.001; scale bar = 20 μm. (B, B' and B'') COS7 cells expressing the constructs indicated were crosslinked with DSP followed by a GFP pull down. Copine 6 content was measured by quantifying Copine 6 antibody signal intensity. Data shown is mean value +/- SEM, N= 3 experiments; \*p<0.05. Copine 6-RFP and Rac1-GFP single (C) and co-transfected (C') COS7 cells with and with out ionomycine incubation. (C'') Copine 6-RFP co-transfected with either Cdc42-GFP or RhoA-GFP in both paradigms incubation with ionomycine was performed scale bar = 20 μm.



---

## Discussion

### Copine 6 expression indicates a postsynaptic function

In the first part of our work, we show evidence for Copine 6 expression coincides spatially and temporally with synaptically dynamic structures. Synapse formation can be described as a gradual accumulation of pre- and postsynaptic components during the second week *in vitro* (**Fig. 10**) that is accompanied by changes in gene transcription. We showed that expression of Copine 6 is upregulated on the mRNA and the protein level during the formation of excitatory synapses in primary hippocampal neurons (**Fig. 11A, B**). Importantly, recent data shows that the temporal expression pattern of genes relevant for synapse function highly correlate in the developing hippocampus *in vitro* and *in vivo* [93, 94]. In support of this notion, we provide evidence for expressional upregulation of Copine 6 during the developmental interval related to synaptogenesis *in vivo* (**Fig. 11B, right**). Synaptogenesis peaks during early development in order to establish a neuronal network but remains at lower levels throughout life. Analysis of Copine 6 expression in the adult rat brain revealed that Copine 6 expression levels spatially correlate with levels of plasticity (**Fig. 11C, D**). The olfactory bulb granule cells are continuously renewed throughout life. With more than 30,000 newborn granule cells reaching the adult rodent olfactory bulb every day, it undergoes continuous synaptic plasticity at a high rate [95, 96]. Also, the hippocampus relies on synaptic plasticity for long term memory and spatial navigation. Together, this provides evidence that Copine 6 expression coincides with neurons undergoing high synaptic turnover. Intriguingly, Copine 6 expression in hippocampal neurons is upregulated upon kainate injection and after induction of long term potentiation (LTP), showing that Copine 6 can also dynamically change its expression level [62]. Importantly, the subcellular localization of Copine 6 in primary hippocampal neurons shows that Copine 6 expression not only coincides in cells undergoing synaptic rearrangements, but enriches in structures (ie. spines) undergoing these rearrangements (**Fig. 11E, F**), clearly linking Copine 6 to activity-induced postsynaptic rearrangements.

### Calcium triggers translocation of Copine 6 to lipid rafts

Homogenates which we treated with changing calcium concentration indicate that calcium induces binding of Copine 6 to plasma membranes (**Fig. 12A**). Intriguingly, the concentration which was required for binding to plasma membranes was roughly around 5  $\mu$ M of calcium

---

(**Fig. 12B**). This is of particular importance, as membrane binding is one order of magnitude above intracellular calcium suggesting cytosolic presentation at basic conditions [97]. Closer analysis revealed that membrane binding was not ubiquitous but restricted to puncta which turned out to be cholesterol-rich lipid rafts (**Fig. 13A**). Interestingly, subcellular fractionation of adult rat brain showed that spines are enriched for lipid raft markers like Flotillin-1 (**Fig. 13B**), explaining Copine 6 enrichment to spines observed in organotypic slice cultures. Lipid rafts are known for its inertia. Lateral diffusion of phospholipids out of spines occurs under normal condition within less than 10 seconds [98]. As other Copine family members have been described to bind selectively to negatively charged phospholipids like phosphatidylserine (PS), phosphatidylglycerol (PG), phosphatidylinositol (PI) and phosphatidic acid (PA), one attractive model is that lipid rafts provide a static environment with different electrostatic properties than the surrounding plasma membrane. In consequence, application of cyclodextrin may disperse these docking sites and avert the ability of Copine 6 to bind upon changes in calcium concentration (**Fig. 13D and D'**).

### **Copine 6 translates synaptic activity to spine stability**

NMDA receptors activation is pivotal for Copine 6 translocation to the plasma membrane and in particular to spines (**Fig. 14B**). A unique property of the NMDA receptor is its voltage-dependent activation, putting downstream events in juxtaposition with synaptic plasticity. Binding of Copine 6 to the plasma membrane and spines was reversible (**Fig. 12A and 14A**) and translocation to the membrane required 5  $\mu$ M cytosolic calcium and occurred only 5 minutes after calcium levels were elevated (**Fig. 15A**). Interestingly, this describes all features of a low pass filter, translating sustained synaptic activity but not individual events to protein translocation. Since enrichment of Copine 6 at the spine likely induces structural rearrangements, this may reflect a mechanism how individual synapses may integrate changing rates of synaptic activity into structural rearrangements. Importantly, the calcium-insensitive mutant suggests that Copine 6 may not only translate to synapse formation but also to its degradation. Additionally, we find that the knockdown of Copine 6 increase the number of functional synapses, as identified by both changes in pre- and postsynaptic markers (**Fig. 17A, C, E**) and increase the frequency of miniature EPSCs (**Fig. 17D**). Importantly, co-expression of shRNA directed against Copine 6 together with a Copine 6 Rescue-Construct which is not targeted by the shRNA reversed the observed effects thus proving evidence that the effects described above were specific to loss of Copine 6 (**Fig. 17B**). In contrast, overexpression of Copine 6 in primary hippocampal neurons caused no effect (**Fig. 18**). As Copine 6 translocates in a calcium-dependent manner but has no enzymatic function by itself, these results further support that Copine 6 acts as a shuttle

---

protein. In accordance with this notion, overexpression does not interfere with the function of the endogenous Copine 6. However, overexpression of a calcium-insensitive Copine 6 mutant which remains in the cytosol competed with the shuttling, endogenous Copine 6 for this target protein and mimicked low synaptic activity and caused a loss of functional synapses (**Fig. 19**).

### **Copine 6 regulates synapse number via Rac1**

We provided evidence that Rac1 is the target protein. Application of NSC 23766, a Rac1 specific inhibitor which is blocking the Kalirin-7 and Tiam-1 GTP exchange sites averted changes induced by shRNA to Copine 6 and mimicked the phenotype induced by the calcium-insensitive Copine 6 (**Fig. 20A**). Furthermore, we show direct interaction between Rac1 and Copine 6 which does not depend on calcium binding to Copine 6 or the activity state of Rac1 (**Fig. 20B**). Additionally we observed Copine 6-dependent translocation of Rac1 in COS cells upon treatment with ionomycin which was absent when Rac1 was expressed alone (**Fig. 20C and C'**). The Copine 6 mediated and calcium dependent translocation was not observed for other Rho like GTPases like Cdc42 or RhoA (**Fig. 20C''**). In summary, this supports our notion that Copine 6 plays a pivotal role translating synaptic activity to Rac1 dependent structural rearrangements. Rac1 remains bound to Copine 6 in the cytosol in low calcium conditions, while synaptic activity-dependent increase in calcium concentration caused translocation of Rac1 to the spine and in consequence triggered structural rearrangements (**Fig. 21**). In support of this view, Rac1 has been described to locate to rafts in neurons [99], and we show that Copine 6 is directly necessary and sufficient for translocation of Rac1 to these structures in a calcium-dependent manner. Taken together, we are the first to show that regulating the availability of a GTPase itself provides a powerful way to achieve phenotypical changes. In conclusion, we believe that understanding the molecular mechanisms underlying an event reflects not only knowing the players but also its location at any given time.

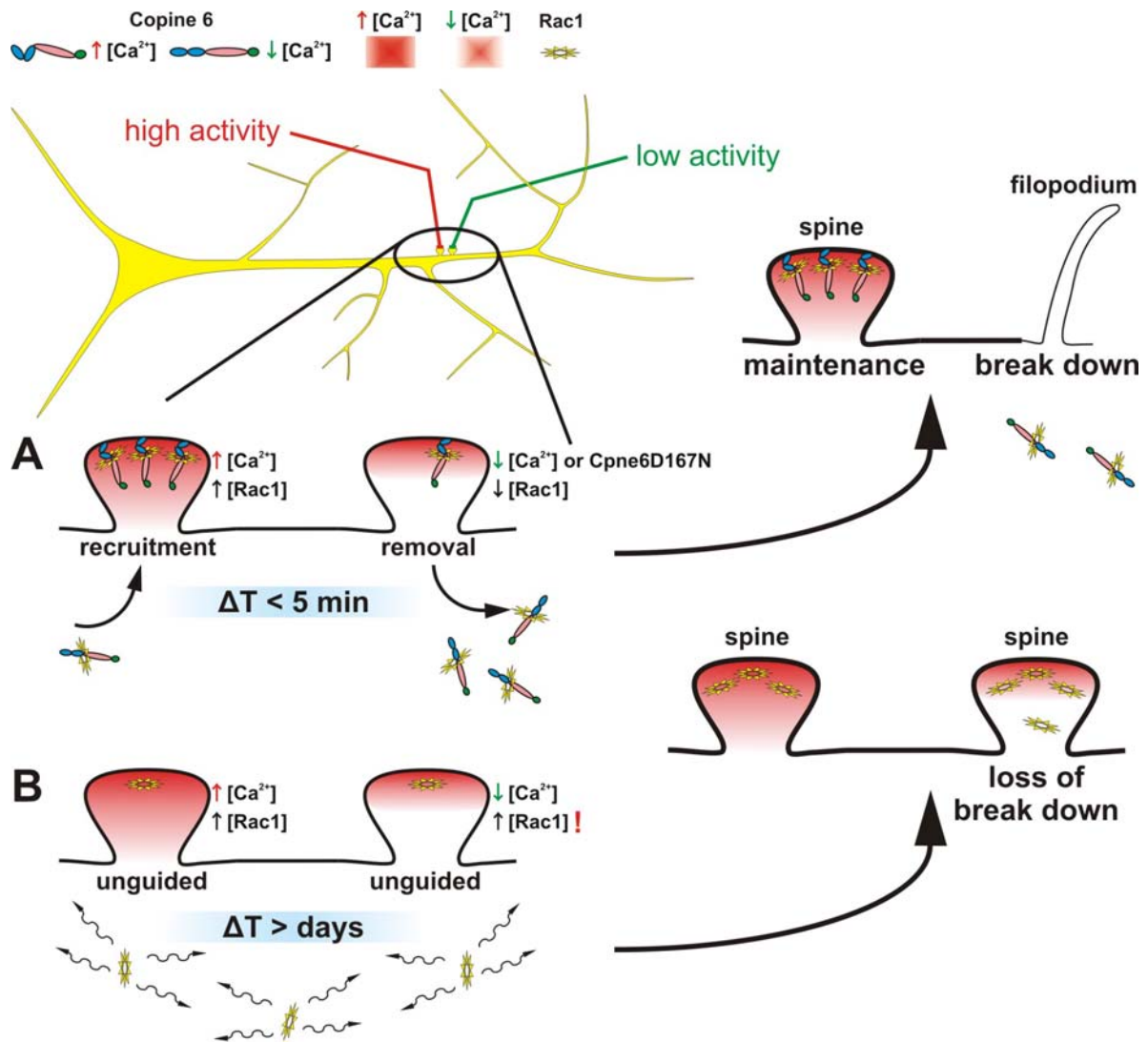


**Figure 21: Action of the Copine 6-Rac1 complex in activity dependent spine morphology**

In neurons, the Copine 6-Rac1 complex acts as a regulator of synaptic stability. **(A, left synapse)** A synapse which is involved in highly active networking, is enriched with Copine6-Rac1 within minutes, which cause a stabilization of this particular synapse. **(A, right synapse)** In immediate proximity, a synapse is removed from a network and its activity level drops. This causes also the decrease of calcium concentration in the spine which results in the removal of Copine 6-Rac1, subsequently depleting the synapse of Rac1. Finally the synapse is undergoing a transition to become a filopodium, a spine precursor. This is also observed when a calcium-insensitive Copine 6 mutant is expressed.

**(B)** In case of loss of Copine 6, Rac1 diffuses unguided through the cell. Within days, independent of calcium and activity, Rac1 can be also found in spines. Because Copine 6 is missing the neuron loses its Rac1 removal mechanism which results in the loss of spine break down and finally an increase in synapses.

---

## Materials and Methods

### DNA constructs and antibodies

All shRNA constructs were designed according to Elbashir et al. (Elbashir, 2001) and cloned under a U6 promotor into a SK(-)-vector. All shRNAs target the open reading frame. Sequences for the sense strand of the central 21-nt double-stranded region are the following: for shRNA to CD4: 5'-CTCTAACCCCTTGACAGAGT-3'; the two used to target Copine 6 were: shRNA to Copine 6-1: 5'-GGAGATCTATAAGACCAATGG-3'; shRNA to Copine 6-2: 5'-GCAAGTCCACTATCACGATCG-3'. A shRNA Copine 6-1 resistant Copine 6 construct was generated by replacing the shRNA recognition sequence with a synthetic nucleotide stretch of silent mutations to: GGAAATATACAAAACAAACGG. Overexpression constructs were cloned into pEGFP(N3), pEGFP(C1), pIRES2-EGFP (BD Bioscience, Clontech), pcDNA3-1(+) and pcDNA3.1(-) (Invitrogen), pMH4 (gift from Thomas Oertner, FMI). The following Primers were used for construct cloning: Copine 6: ss *HindIII* 5'-cccaagcttagtgccatgtcggaccagagatgggatgggtgcctgagc-3' and as *BamHI* 5'-cgcggatcctgggctgggctggg-3' for fusion to GFP and for IRES plus STOP as *BamHI* 5'-cgcggatcctcatgggctgggctggg-3',  $\beta$ -actin: ss *EcoRI* 5'-ccggaattcttcgccatggatgac-3' and as *BamHI* 5'-cgcggatccgaagcatttgcggtgcac-3'. Rac1V12GFP was generated from a wt template by single primer mutagenesis using: 5'-agacgtaagctgttgtaaaact-3'. Rac1N17GFP was generated from a wt template by single primer mutagenesis using: 5'-agacggagctgttgtaaaaact-3'. Following antibodies were used: PSD95 (ABR, MA1-045), SynGAP (ABR, PA1-046), N-Copine (BD Bioscience, CG8695), Tubulin (BD Bioscience, 556321), MAP2 (Chemicon, AB5622), GFP (Chemicon, AB16901), Bassoon (Stressgen, VAM-PS003), GluR2 (BD Bioscience, 556341), Flotillin-1 (BD Bioscience, 610820).

### Quantitative real-time PCR.

The real-time PCR was carried out on an ABI 7000 and 7700 Sequence Detection system (Applied Biosystems). Primer sequences were designed using Primer Express software (PE; Applied Biosystems). We selected primers close to the 3' end of the target genes with primers localized on different exons. Amplicons were 150 bp ( $\pm$  10%) in size. Primers were: Copine 6s: (5'-CCCCAAGTACCGAGACAAGAAGA-3'); Copine 6as: (5'-GGAGGCTGTGAAGTCGATAGC-3'); GAPDHs: (5'-CATCGTGGAAGGGCTCATGAC-3'); GAPDHs: (5'-CTTGGCAGCACCAAGTGGATG-3'); PGK 1s: (5'-GCCCATGCCCGACAAGTAC-3'); PGK 1as: (5'-GAGGTTCTCCAGGAGGATGAC-3');

---

SynGAPs: (5'- GCCAGAAATACCTCAAGGATGCC-3'); SynGAPs: (5'- GCACAGGGCCAACTCACAG-3'). The reactions were all performed using the SYBR Green PCR Core Reagents (Applied Biosystems).

### **Pharmacological agents and inhibitors**

Glutamic acid (Sigma Aldrich, Prod.No.: G-2128) [10 mM] stock solution, set to [50  $\mu$ M] as reaction concentration; NMDA (Tocris, Prod.No.: 0114) [100 mM] stock solution, set to [10  $\mu$ M] reaction concentration; D-APV (Tocris, Prod.No.: 0106) [10 mM] stock solution, set to [50  $\mu$ M] reaction concentration; trans ACBD (Tocris, Prod.No.: 0270) [100 mM] stock solution, set to [50  $\mu$ M] reaction concentration; CdCl<sub>2</sub> (Sigma Aldrich, Prod.No.: 655198) [100 mM], set to [50  $\mu$ M] reaction concentration; NSC 23766 (Tocris, Prod.No.: 2161) [50 mM], set to [100  $\mu$ M] reaction concentration.

### **Primary hippocampal cultures**

Low density cultures ( $\sim$ 150 cells mm<sup>-2</sup>) were used for co-localization studies and expression profile experiments. Hippocampal cultures were established from 18 day old fetal Wistar rat hippocampi and primary astrocytes, used as feeder layer, were obtained from newborn rat cortical hemisphere. For functional and morphological studies, high density hippocampal primary neuronal cultures were used. The hippocampi were dissected from embryonic day (E) 18–19 rat embryos and washed in ice cold HBSS buffer followed by 15 min incubation in trypsin at 37°C. After a second wash with HBSS hippocampi were additionally washed in prewarmed DMEM complete plating medium containing 0.6% glucose. Dissociation was performed in prewarmed plating medium and plated at high density ( $\sim$ 750 cells mm<sup>-2</sup>) on glass slides (pre coated with poly-L-lysine o/n followed by extensive washing with PBS). After 3 h plating medium was exchanged with culture medium containing: Neurobasal medium (Gibco), [0.5 mM] glutamine, antibiotics and B27 supplement (Gibco). Experiments were performed in accordance with the Federal Ordinance on the Protection of Animals.

### **Transfection, Immunocytochemistry**

Transfection of hippocampal culture was performed in 24-well-plates using Lipofectamine2000 following the manufacturer's instructions at DIV 7 with a total of 500 ng DNA for a 24 well plate of neurons (shRNA:GFP 4:1; shRNA:GFP: $\beta$ -actin 4:0.5:0.5; CpneX-GFP: $\beta$ -actin 4:1). Neuronal cells were fixed between DIV 12 and DIV 14 with 4%

---

paraformaldehyde in PBS with 120 mM sucrose, permeabilized with 0.25% Triton X-100 in PBS and, subsequently incubated with primary antibody overnight at 4°C in PBS with 3% BSA. Finally, cells were treated with appropriate secondary antibody for 1 h at RT and the immunolabeled cells were mounted with Cervol.

### **Ionomycin treatment**

Ionomycin (Sigma Aldrich; I9657) was dissolved in DMSO and diluted to 2 µM in empty DMEM. 24 h post transfected COS7 cells were washed twice with prewarmed PBS and incubated for 5 min in 2 µM ionomycin at 37°C. After washing in PBS cells were fixed with 4% PFA in PBS for 30 min.

### **Lipid raft staining**

COS 7 cells were fixed and subsequently stained for lipid rafts with 1 µg/ml Cholera toxin subunit B1 (Molecular probes; C-34778 conjugated with Alexa 647) for 1 h at RT. After washing with PBS glass slides were mounted and analysed.

### **Imaging**

Pictures were made on Leica DM5000 and analyzed using the “analySIS” software or in case of picture stacks with the Leica SPE or Leica SP5 system.

### **Cholesterol depletion**

COS7 cells expressing Copine 6-GFP for 24 h were washed twice with prewarmed PBS followed by an incubation with 10 mM Cyclodextrin (Sigma Alrich; Prod.Nr.: C4555) in empty DMEM for 1 h at 37°C. After washing twice with ice cold PBS cells were scraped and subjected for further analysis.

### **Lipid raft isolation**

According to Hering et al. Journal of Neuroscience 2003, 1 adult rat brain was split into left and right hemisphere. Each hemisphere was homogenized in 2 ml of either TNXC + [5 mM] CaCl<sub>2</sub> or TNXE + [5 mM] EDTA; TNX buffer: [25 mM] Tris pH 7.5; [320 mM] Sucrose; [150



---

mM] NaCl; 1% TX-100; Roche proteinase inhibitors by a motorized glas/teflon homogenizer 15 strokes, full speed. Debris was removed by 800 x g for 10 min at 4°C. The supernatant was further spun with 10.200 x g for 15 min at 4°C and the pellet resuspended in either TNE + [5 mM] EDTA or TNC + [5 mM] CaCl<sub>2</sub>; TN buffer [50 mM] Tris pH 7.5; [150 mM] NaCl; Roche complete protease inhibitors. The resuspended pellet was sonicated for 5 sec at 4°C (MSE sonicator; amplitude stage 4; intensity low) and 0.1 vol of 10 x TNX(C/E) was added and mixed. After rotating for 20 min at 4°C the sample was adjusted to 45% sucrose by adding half of the total volume of 90%. Overlay the 45% sucrose sample with 12 ml of a linear sucrose gradient (35%-5% in TNE/C; cast by using stirrer columns). Centrifuge with 100.000 x g for 20 h at 4°C to cause floating of lipidraft fractions.

### **Subcellular fractionation of COS7 cells**

A 10 cm (56 cm<sup>2</sup>) dish COS7 cells was transfected as a 40-50% confluent culture with 2.5 µg of DNA. After 24 h cells were washed 2x with ice cold PBS and scraped in 500 µl ice cold CLB buffer: [10 mM] Hepes, [10 mM] NaCl, [1 mM] KH<sub>2</sub>PO<sub>4</sub>, [5 mM] NaHCO<sub>3</sub>, [0.5 mM] MgCl<sub>2</sub> and Roche complete protease inhibitors in presence or absence of either [1 mM] CaCl<sub>2</sub>, [10 nM] EGTA or [2 mM] EDTA. After homogenization in a motorized teflon/glas homogenizer (300 rpm, 10 strokes) 50 µl of 2.5 M sucrose was added and carefully mixed by pipetting up and down. Nuclei and cell debris were removed by an initial centrifugation (6300 x g, 4°C, 5 min) and the supernatant was distributed in 200 µl aliquots. Each aliquot was set to the appropriate CaCl<sub>2</sub>, EGTA or EDTA concentration and incubated in head over head shaker for 15 min at 4°C. Membrane (M) and cytoplasmis (C) fractions were separated by spinning the aliquots with 100.000 x g, 4°C, 30 min in a TST 41.14 rotor. The 200 µl supernatant was removed and the pellet diluted in 200 µl CLB (or aliquot volume) buffer followed by cooking in Laemmlibuffer for 10 min at 96°C.

### **PSD fractionation and isolation of rat brains**

Following guide lines were modified from "B.D.Lynn et al. Brain Research 898(2001)1-8". 1 adult rat brain (2g) was homogenized in 10 volumes of ice-cold buffer A: [0.32 M] sucrose, [1 mM] NaHCO<sub>3</sub>, [1 mM] MgCl<sub>2</sub>, [0.5 mM] CaCl<sub>2</sub>) with 12 strokes of a motor-driven (800 rpm) Teflon-glass homogenizer. The homogenate was centrifuged at 1400 x g for 10 min (SS34, 10500 rpm 4°C), the nuclear pellet was resuspended (+/- 2 mM EDTA) and centrifuged. The post-nuclear supernatants were combined and centrifuged at 13,800xg 10 min 4°C to yield a synaptosomal-mitochondrial pellet (P2). The supernatant of P2 was centrifuged at 100,000xg for 2 h to obtain a pellet consisting of microsomal and plasma membranes (P3 fraction). P2

---

was resuspended in buffer A (+/- 2 mM EDTA), layered onto a discontinuous 0.85 M, 1.0 M and 1.2 M sucrose density gradient containing 1 mM NaHCO<sub>3</sub>, centrifuged at 82,500 × g for 2 h using a TST 41.14 rotor, and the subfraction located at the 1.0 M - 1.2 M sucrose density interface were collected. This crude synaptosome fraction was diluted in 4x vol. buffer B and after resuspension was then centrifuged at 13.800×g for 10 min at 4°C the pellet, containing Triton-insoluble material (Pre-PSD), was resuspended in buffer C: [10 mM] Hepes, (+/- 0.5 mM CaCl<sub>2</sub> and +/- 2 mM EDTA) + Roche complete Protease Inhibitors. After 15 min at 4°C hypotonic lysis occurred and Synaptic membranes (SM) were pelleted by spinning the sample with 13.800g for 10 min at 4°C in an eppendorf table top centrifuge. The supernatant (S5) was stored as synaptosomal cytoplasm whereas the SM fraction was further incubated in [10 mM] Hepes, [150 mM] NaCl, 2%TX-100 for 15 min rotating at 4°C followed by a 100.000xg centrifugation for 30 min at 4°C resulting in postsynaptic densities (PSD) and S6. Protein concentration was measured and equal amounts of protein subjected for Immunoblotting.

### **Life imaging**

18mm glas slides covered with DIV 14 neurons transfected with Copine 6-GFP and tdRFP were transferred from a 12 well plate into a life imaging chamber (Ludin) into a low MgCl<sub>2</sub> prewarmed ringer solution: [135 mM] NaCl, [3 mM] KCl, [2 mM] CaCl<sub>2</sub>, [10 mM] Hepes, [2 mM] MgSO<sub>4</sub>, [25 mM] Glucose, [20 µM] Glycine (pH 7,3 - 7,4, 320 mOsm). After 20 min at 37°C the chamber was placed in a prewarmed Zeiss, Axiovert 135M Microscope. The ringersolution in the chamber was replaced to the [10 µM] NMDA condition by two syringes followed by taking pictures every 30 sec for total time of 20 min.

### **Electrophysiology**

High density cultures (DIV12) were perfused with an ACSF solution containing (in mM): 119 NaCl, 2.5 KCl, 1.3 MgCl<sub>2</sub>, 2.5 CaCl<sub>2</sub>, 1 NaH<sub>2</sub>PO<sub>4</sub>, 26.2 NaHCO<sub>3</sub>, 11 glucose, equilibrated with 95%O<sub>2</sub>/5%CO<sub>2</sub> at room temperature (25°C) and delivered at 1.5ml per min. Whole-cell patch-clamp recordings were performed from the somata of visually identified neurons. The recording electrode (3-5MΩ) was filled with a solution containing (in mM): 135 CsMeSO<sub>4</sub>, 8 NaCl, 10 HEPES, 0.5 EGTA, 5 QX-314, 4 Mg-ATP, 0.3 Na-GTP (pH 7.25, 285 mOsm). Miniature EPSC (mEPSCs) were recorded at -70mV in the presence of 0.5µM TTX (Latoxan, Valence, France) and 100µM picrotoxin (Fluka/Sigma, Buchs, Switzerland). Detection and analysis of mEPSCs were done using the MiniAnalysis software (Synaptosoft, Decatur, GA,

---

USA). 600 consecutive events from each cell were used for the cumulative probability graph and the Kolmogorov-Smirnov tests. Data were obtained with an Axopatch 200B (Axon Instruments, Union City, CA, USA), filtered at 2 kHz and digitized at 10 kHz, acquired and analyzed with pClamp9 (Axon Instruments, Union City, CA, USA).

### **Two-photon laser imaging**

In all experiments, organotypic slice cultures were obtained from Wistar rats at postnatal day 5. Slices were transfected between day in vitro 5 to 7 using a biolistic gene gun. After transfections, the cultures appeared healthy, and the expression of Copine-GFP and RFP was analyzed under epifluorescence illumination between DIV21-DIV28. We used a custom-built 2-photon laser scanning microscope (2PLSM) based on a Olympus BX51WI microscope with LUMPlan 60x/0.90 objective, and a Ti:sapphire laser tuned to  $\lambda = 910$  nm for excitation. Fluorescence was detected using photomultiplier tubes. Image acquisition was controlled by custom software (MatLab7).

### **Immunoprecipitation and Western blotting**

10cm dish COS7 cells were transfected as a 40-50% confluent culture and harvested 24 h post-transfection. Cells were lysed in 1ml lysis buffer: [50mM] Tris pH7.5, [150mM] NaCl, 1% NP-40, 0.5% deoxycholate and Roche complete mini protease inhibitors for 20min on ice and insoluble materials were removed by centrifugation at 10,000g for 10 min at 4°C before antibody was applied to the supernatant for immunoprecipitation (2 $\mu$ g of antibody for each IP was used). Brain lysates were prepared from adult rat brains. Olfactory bulb, frontal cortex, motoric cortex, hippocampus, cerebellum and brainstem were dissected and lysed in a weight:vol 1:10 ratio in RIPA buffer + Roche complete mini protease inhibitors. Tissues were passed 10 times through a 25G syringe and incubated for 20min on ice. Insoluble materials were removed by centrifugation at 10,000g for 10 min at 4°C. Equal amounts of protein were separated by 10% PAGE, transferred to nitrocellulose membrane, and immuno-stained using antibodies previously described. After estimating the proper  $\beta$ -actin ratios samples were adjusted to the house keeper and reloaded.

### **Crosslinking**

24 h post transfected cells were washed twice with prewarmed PBS. After washing cells were incubated with 2 mM Dithiobis succinimidyl propionate (DSP; Pierce; Prod.Nr.: 22585) in PBS (derived from diluting a 25 mM DSP DMSO stock solution (freshly prepared) with

---

PBS. After incubation on ice for 2 h, the reaction was stopped by adding 1 M Tris pH 7.5 to a final concentration of 20 mM followed by a further incubation of 15 min on ice

---

## References

1. Togashi, H., et al., *Cadherin regulates dendritic spine morphogenesis*. *Neuron*, 2002. **35**(1): p. 77-89.
2. Chavis, P. and G. Westbrook, *Integrins mediate functional pre- and postsynaptic maturation at a hippocampal synapse*. *Nature*, 2001. **411**(6835): p. 317-21.
3. Scheiffele, P., et al., *Neurologin expressed in nonneuronal cells triggers presynaptic development in contacting axons*. *Cell*, 2000. **101**(6): p. 657-69.
4. Biederer, T., et al., *SynCAM, a synaptic adhesion molecule that drives synapse assembly*. *Science*, 2002. **297**(5586): p. 1525-31.
5. Penzes, P., et al., *Rapid induction of dendritic spine morphogenesis by trans-synaptic ephrinB-EphB receptor activation of the Rho-GEF kalirin*. *Neuron*, 2003. **37**(2): p. 263-74.
6. Pin, J.P. and R. Duvoisin, *The metabotropic glutamate receptors: structure and functions*. *Neuropharmacology*, 1995. **34**(1): p. 1-26.
7. Hollmann, M. and S. Heinemann, *Cloned glutamate receptors*. *Annu Rev Neurosci*, 1994. **17**: p. 31-108.
8. Ehlers, M.D., et al., *Synaptic targeting of glutamate receptors*. *Curr Opin Cell Biol*, 1996. **8**(4): p. 484-9.
9. Pawson, T. and J.D. Scott, *Signaling through scaffold, anchoring, and adaptor proteins*. *Science*, 1997. **278**(5346): p. 2075-80.
10. Sheng, M. and D.T. Pak, *Glutamate receptor anchoring proteins and the molecular organization of excitatory synapses*. *Ann N Y Acad Sci*, 1999. **868**: p. 483-93.
11. Harris, K.M. and S.B. Kater, *Dendritic spines: cellular specializations imparting both stability and flexibility to synaptic function*. *Annu Rev Neurosci*, 1994. **17**: p. 341-71.
12. Okabe, S., A. Miwa, and H. Okado, *Spine formation and correlated assembly of presynaptic and postsynaptic molecules*. *J Neurosci*, 2001. **21**(16): p. 6105-14.
13. Marrs, G.S., S.H. Green, and M.E. Dailey, *Rapid formation and remodeling of postsynaptic densities in developing dendrites*. *Nat Neurosci*, 2001. **4**(10): p. 1006-13.
14. Parnass, Z., A. Tashiro, and R. Yuste, *Analysis of spine morphological plasticity in developing hippocampal pyramidal neurons*. *Hippocampus*, 2000. **10**(5): p. 561-8.
15. Harris, K.M., *Structure, development, and plasticity of dendritic spines*. *Curr Opin Neurobiol*, 1999. **9**(3): p. 343-8.
16. Friedman, H.V., et al., *Assembly of new individual excitatory synapses: time course and temporal order of synaptic molecule recruitment*. *Neuron*, 2000. **27**(1): p. 57-69.
17. Ahmari, S.E., J. Buchanan, and S.J. Smith, *Assembly of presynaptic active zones from cytoplasmic transport packets*. *Nat Neurosci*, 2000. **3**(5): p. 445-51.

- 
18. Sans, N., et al., *A developmental change in NMDA receptor-associated proteins at hippocampal synapses*. J Neurosci, 2000. **20**(3): p. 1260-71.
  19. Washbourne, P., J.E. Bennett, and A.K. McAllister, *Rapid recruitment of NMDA receptor transport packets to nascent synapses*. Nat Neurosci, 2002. **5**(8): p. 751-9.
  20. Schneggenburger, R. and E. Neher, *Intracellular calcium dependence of transmitter release rates at a fast central synapse*. Nature, 2000. **406**(6798): p. 889-93.
  21. Bollmann, J.H. and B. Sakmann, *Control of synaptic strength and timing by the release-site Ca<sup>2+</sup> signal*. Nat Neurosci, 2005. **8**(4): p. 426-34.
  22. Sudhof, T.C., *The synaptic vesicle cycle*. Annu Rev Neurosci, 2004. **27**: p. 509-47.
  23. Geppert, M., et al., *Synaptotagmin I: a major Ca<sup>2+</sup> sensor for transmitter release at a central synapse*. Cell, 1994. **79**(4): p. 717-27.
  24. Fernandez-Chacon, R., et al., *Synaptotagmin I functions as a calcium regulator of release probability*. Nature, 2001. **410**(6824): p. 41-9.
  25. Maletic-Savatic, M., R. Malinow, and K. Svoboda, *Rapid dendritic morphogenesis in CA1 hippocampal dendrites induced by synaptic activity*. Science, 1999. **283**(5409): p. 1923-7.
  26. Linden, D.J., *Long-term synaptic depression in the mammalian brain*. Neuron, 1994. **12**(3): p. 457-72.
  27. Malenka, R.C. and R.A. Nicoll, *Long-term potentiation--a decade of progress?* Science, 1999. **285**(5435): p. 1870-4.
  28. Nagerl, U.V., et al., *Bidirectional activity-dependent morphological plasticity in hippocampal neurons*. Neuron, 2004. **44**(5): p. 759-67.
  29. Zhou, Q., K.J. Homma, and M.M. Poo, *Shrinkage of dendritic spines associated with long-term depression of hippocampal synapses*. Neuron, 2004. **44**(5): p. 749-57.
  30. Lee, H.K., et al., *Regulation of distinct AMPA receptor phosphorylation sites during bidirectional synaptic plasticity*. Nature, 2000. **405**(6789): p. 955-9.
  31. Isaac, J.T., R.A. Nicoll, and R.C. Malenka, *Evidence for silent synapses: implications for the expression of LTP*. Neuron, 1995. **15**(2): p. 427-34.
  32. Liao, D., N.A. Hessler, and R. Malinow, *Activation of postsynaptically silent synapses during pairing-induced LTP in CA1 region of hippocampal slice*. Nature, 1995. **375**(6530): p. 400-4.
  33. Manahan-Vaughan, D., et al., *A single application of MK801 causes symptoms of acute psychosis, deficits in spatial memory, and impairment of synaptic plasticity in rats*. Hippocampus, 2008. **18**(2): p. 125-34.
  34. Lee, S.J., et al., *Activation of CaMKII in single dendritic spines during long-term potentiation*. Nature, 2009. **458**(7236): p. 299-304.
  35. Derkach, V.A., et al., *Regulatory mechanisms of AMPA receptors in synaptic plasticity*. Nat Rev Neurosci, 2007. **8**(2): p. 101-13.

- 
36. Photowala, H., et al., *G protein betagamma-subunits activated by serotonin mediate presynaptic inhibition by regulating vesicle fusion properties*. Proc Natl Acad Sci U S A, 2006. **103**(11): p. 4281-6.
  37. Lisman, J. and S. Raghavachari, *A unified model of the presynaptic and postsynaptic changes during LTP at CA1 synapses*. Sci STKE, 2006. **2006**(356): p. re11.
  38. Fukazawa, Y., et al., *Hippocampal LTP is accompanied by enhanced F-actin content within the dendritic spine that is essential for late LTP maintenance in vivo*. Neuron, 2003. **38**(3): p. 447-60.
  39. Meng, Y., et al., *Abnormal spine morphology and enhanced LTP in LIMK-1 knockout mice*. Neuron, 2002. **35**(1): p. 121-33.
  40. Honkura, N., et al., *The subspine organization of actin fibers regulates the structure and plasticity of dendritic spines*. Neuron, 2008. **57**(5): p. 719-29.
  41. Matsuzaki, M., et al., *Structural basis of long-term potentiation in single dendritic spines*. Nature, 2004. **429**(6993): p. 761-6.
  42. Harvey, C.D. and K. Svoboda, *Locally dynamic synaptic learning rules in pyramidal neuron dendrites*. Nature, 2007. **450**(7173): p. 1195-200.
  43. Watabe-Uchida, M., E.E. Govek, and L. Van Aelst, *Regulators of Rho GTPases in neuronal development*. J Neurosci, 2006. **26**(42): p. 10633-5.
  44. Kozma, R., et al., *Rho family GTPases and neuronal growth cone remodelling: relationship between increased complexity induced by Cdc42Hs, Rac1, and acetylcholine and collapse induced by RhoA and lysophosphatidic acid*. Mol Cell Biol, 1997. **17**(3): p. 1201-11.
  45. Bishop, A.L. and A. Hall, *Rho GTPases and their effector proteins*. Biochem J, 2000. **348 Pt 2**: p. 241-55.
  46. Tashiro, A. and R. Yuste, *Role of Rho GTPases in the morphogenesis and motility of dendritic spines*. Methods Enzymol, 2008. **439**: p. 285-302.
  47. Tashiro, A., A. Minden, and R. Yuste, *Regulation of dendritic spine morphology by the rho family of small GTPases: antagonistic roles of Rac and Rho*. Cereb Cortex, 2000. **10**(10): p. 927-38.
  48. Thalhammer, A., et al., *CaMKII translocation requires local NMDA receptor-mediated Ca<sup>2+</sup> signaling*. Embo J, 2006. **25**(24): p. 5873-83.
  49. Saneyoshi, T., et al., *Activity-dependent synaptogenesis: regulation by a CaM-kinase kinase/CaM-kinase I/betaPIX signaling complex*. Neuron, 2008. **57**(1): p. 94-107.
  50. Park, E., et al., *The Shank family of postsynaptic density proteins interacts with and promotes synaptic accumulation of the beta PIX guanine nucleotide exchange factor for Rac1 and Cdc42*. J Biol Chem, 2003. **278**(21): p. 19220-9.
  51. Maekawa, M., et al., *Signaling from Rho to the actin cytoskeleton through protein kinases ROCK and LIM-kinase*. Science, 1999. **285**(5429): p. 895-8.
  52. Schubert, V., J.S. Da Silva, and C.G. Dotti, *Localized recruitment and activation of RhoA underlies dendritic spine morphology in a glutamate receptor-dependent manner*. J Cell Biol, 2006. **172**(3): p. 453-67.



- 
53. Creutz, C.E., et al., *The copines, a novel class of C2 domain-containing, calcium-dependent, phospholipid-binding proteins conserved from Paramecium to humans*. J Biol Chem, 1998. **273**(3): p. 1393-402.
  54. Rizo, J. and T.C. Sudhof, *C2-domains, structure and function of a universal Ca<sup>2+</sup>-binding domain*. J Biol Chem, 1998. **273**(26): p. 15879-82.
  55. Sudhof, T.C. and J. Rizo, *Synaptotagmins: C2-domain proteins that regulate membrane traffic*. Neuron, 1996. **17**(3): p. 379-88.
  56. Orita, S., et al., *Doc2: a novel brain protein having two repeated C2-like domains*. Biochem Biophys Res Commun, 1995. **206**(2): p. 439-48.
  57. Tomsig, J.L. and C.E. Creutz, *Biochemical characterization of copine: a ubiquitous Ca<sup>2+</sup>-dependent, phospholipid-binding protein*. Biochemistry, 2000. **39**(51): p. 16163-75.
  58. Cowland, J.B., et al., *Tissue expression of copines and isolation of copines I and III from the cytosol of human neutrophils*. J Leukoc Biol, 2003. **74**(3): p. 379-88.
  59. Tomsig, J.L., S.L. Snyder, and C.E. Creutz, *Identification of targets for calcium signaling through the copine family of proteins. Characterization of a coiled-coil copine-binding motif*. J Biol Chem, 2003. **278**(12): p. 10048-54.
  60. Greene, N.D., et al., *Differential protein expression at the stage of neural tube closure in the mouse embryo*. J Biol Chem, 2002. **277**(44): p. 41645-51.
  61. Ding, X., et al., *Localization and cellular distribution of CPNE5 in embryonic mouse brain*. Brain Res, 2008. **1224**: p. 20-8.
  62. Nakayama, T., et al., *N-copine: a novel two C2-domain-containing protein with neuronal activity-regulated expression*. FEBS Lett, 1998. **428**(1-2): p. 80-4.
  63. Nakayama, T., T. Yaoi, and G. Kuwajima, *Localization and subcellular distribution of N-copine in mouse brain*. J Neurochem, 1999. **72**(1): p. 373-9.
  64. Yuste, R. and D.W. Tank, *Dendritic integration in mammalian neurons, a century after Cajal*. Neuron, 1996. **16**(4): p. 701-16.
  65. Jontes, J.D., J. Buchanan, and S.J. Smith, *Growth cone and dendrite dynamics in zebrafish embryos: early events in synaptogenesis imaged in vivo*. Nat Neurosci, 2000. **3**(3): p. 231-7.
  66. Ziv, N.E. and S.J. Smith, *Evidence for a role of dendritic filopodia in synaptogenesis and spine formation*. Neuron, 1996. **17**(1): p. 91-102.
  67. Dunaevsky, A., et al., *Developmental regulation of spine motility in the mammalian central nervous system*. Proc Natl Acad Sci U S A, 1999. **96**(23): p. 13438-43.
  68. Korkotian, E. and M. Segal, *Regulation of dendritic spine motility in cultured hippocampal neurons*. J Neurosci, 2001. **21**(16): p. 6115-24.
  69. Lendvai, B., et al., *Experience-dependent plasticity of dendritic spines in the developing rat barrel cortex in vivo*. Nature, 2000. **404**(6780): p. 876-81.
  70. Chklovskii, D.B., B.W. Mel, and K. Svoboda, *Cortical rewiring and information storage*. Nature, 2004. **431**(7010): p. 782-8.

- 
71. Wong, W.T., et al., *Rapid dendritic remodeling in the developing retina: dependence on neurotransmission and reciprocal regulation by Rac and Rho*. J Neurosci, 2000. **20**(13): p. 5024-36.
  72. Wong, W.T. and R.O. Wong, *Rapid dendritic movements during synapse formation and rearrangement*. Curr Opin Neurobiol, 2000. **10**(1): p. 118-24.
  73. Yuste, R. and T. Bonhoeffer, *Morphological changes in dendritic spines associated with long-term synaptic plasticity*. Annu Rev Neurosci, 2001. **24**: p. 1071-89.
  74. Sala, C., et al., *Inhibition of dendritic spine morphogenesis and synaptic transmission by activity-inducible protein Homer1a*. J Neurosci, 2003. **23**(15): p. 6327-37.
  75. Hering, H. and M. Sheng, *Activity-dependent redistribution and essential role of cortactin in dendritic spine morphogenesis*. J Neurosci, 2003. **23**(37): p. 11759-69.
  76. Steward, O. and E.M. Schuman, *Protein synthesis at synaptic sites on dendrites*. Annu Rev Neurosci, 2001. **24**: p. 299-325.
  77. Steward, O., *mRNA localization in neurons: a multipurpose mechanism?* Neuron, 1997. **18**(1): p. 9-12.
  78. Zhou, Z., et al., *Brain-specific phosphorylation of MeCP2 regulates activity-dependent Bdnf transcription, dendritic growth, and spine maturation*. Neuron, 2006. **52**(2): p. 255-69.
  79. Yi, J.J. and M.D. Ehlers, *Ubiquitin and protein turnover in synapse function*. Neuron, 2005. **47**(5): p. 629-32.
  80. Colledge, M., et al., *Ubiquitination regulates PSD-95 degradation and AMPA receptor surface expression*. Neuron, 2003. **40**(3): p. 595-607.
  81. Mulkey, R.M., C.E. Herron, and R.C. Malenka, *An essential role for protein phosphatases in hippocampal long-term depression*. Science, 1993. **261**(5124): p. 1051-5.
  82. Steiner, P., et al., *Destabilization of the postsynaptic density by PSD-95 serine 73 phosphorylation inhibits spine growth and synaptic plasticity*. Neuron, 2008. **60**(5): p. 788-802.
  83. Matus, A., *Actin-based plasticity in dendritic spines*. Science, 2000. **290**(5492): p. 754-8.
  84. Calabrese, B. and S. Halpain, *Essential role for the PKC target MARCKS in maintaining dendritic spine morphology*. Neuron, 2005. **48**(1): p. 77-90.
  85. Nakayama, A.Y., M.B. Harms, and L. Luo, *Small GTPases Rac and Rho in the maintenance of dendritic spines and branches in hippocampal pyramidal neurons*. J Neurosci, 2000. **20**(14): p. 5329-38.
  86. Ackermann, M. and A. Matus, *Activity-induced targeting of profilin and stabilization of dendritic spine morphology*. Nat Neurosci, 2003. **6**(11): p. 1194-200.
  87. Damer, C.K., et al., *Copine A, a calcium-dependent membrane-binding protein, transiently localizes to the plasma membrane and intracellular vacuoles in Dictyostelium*. BMC Cell Biol, 2005. **6**: p. 46.

- 
88. Yang, S., et al., *The BON/CPN gene family represses cell death and promotes cell growth in Arabidopsis*. Plant J, 2006. **45**(2): p. 166-79.
  89. Tomsig, J.L., H. Sohma, and C.E. Creutz, *Calcium-dependent regulation of tumour necrosis factor-alpha receptor signalling by copine*. Biochem J, 2004. **378**(Pt 3): p. 1089-94.
  90. Tashiro, A. and R. Yuste, *Regulation of dendritic spine motility and stability by Rac1 and Rho kinase: evidence for two forms of spine motility*. Mol Cell Neurosci, 2004. **26**(3): p. 429-40.
  91. Tolias, K.F., et al., *The Rac1 guanine nucleotide exchange factor Tiam1 mediates EphB receptor-dependent dendritic spine development*. Proc Natl Acad Sci U S A, 2007. **104**(17): p. 7265-70.
  92. Cahill, M.E., et al., *Kalirin regulates cortical spine morphogenesis and disease-related behavioral phenotypes*. Proc Natl Acad Sci U S A, 2009. **106**(31): p. 13058-63.
  93. Dabrowski, M., et al., *Gene profiling of hippocampal neuronal culture*. J Neurochem, 2003. **85**(5): p. 1279-88.
  94. Mody, M., et al., *Genome-wide gene expression profiles of the developing mouse hippocampus*. Proc Natl Acad Sci U S A, 2001. **98**(15): p. 8862-7.
  95. Nissant, A., et al., *Adult neurogenesis promotes synaptic plasticity in the olfactory bulb*. Nat Neurosci, 2009. **12**(6): p. 728-30.
  96. Altman, J., *Autoradiographic and histological studies of postnatal neurogenesis. IV. Cell proliferation and migration in the anterior forebrain, with special reference to persisting neurogenesis in the olfactory bulb*. J Comp Neurol, 1969. **137**(4): p. 433-57.
  97. Carafoli, E., *Intracellular calcium homeostasis*. Annu Rev Biochem, 1987. **56**: p. 395-433.
  98. Craske, M.L., et al., *Spines and neurite branches function as geometric attractors that enhance protein kinase C action*. J Cell Biol, 2005. **170**(7): p. 1147-58.
  99. Kumanogoh, H., et al., *Biochemical and morphological analysis on the localization of Rac1 in neurons*. Neurosci Res, 2001. **39**(2): p. 189-96.

---

## Acknowledgement

I would like to thank my whole family for their support, for believing in me and most of all for their unconditional love. Especially my parents, who always guided me but never forced me to take any decisions. To give a lot and to stand to your word is their way of life and has become mine too. They have always been a secure and constant harbor, where I could return to, no matter how lost I was.

I would like to thank my wife Anja, for always being there for me, literally in good as in bad times. Even in situations when I questioned not only my carrier, she showed the personal strength and greatness of heart to support me. In some situations this meant to act against her love, which is probably the biggest act of love of all.

I thank Markus for providing a scientific frame where I do all my “spiffy” experiments. He created an environment which made it possible to develop a scientific way of thinking and accepted my need for scientific freedom. This resulted in a four year adventure challenging my creativity and intellect.

Special thanks go to my colleagues, who replaced family and friends. They provided emotional security which I had to leave behind when I moved from Vienna to Basel. During my PhD I had to sacrifice some aspects of my life and stress social networks. Nevertheless, I was rewarded by becoming part of a group consisting of people who are trustful, warm hearted and full of joy, and most importantly, some of them even became friends.

Without you all I would be nothing.

---

## Curriculum Vitae:

### ***Personal Information:***

---

Name: Alexander Kriz  
Date of birth: 09.11.1978  
Place of birth: Vienna  
Citizenship: Austrian

### ***Education:***

---

2006/01 – 2009/12 PhD in Neurobiology, University of Basel  
1998/10 – 2004/11 Master of Sciences, graduate study of biology, University of Vienna  
1997/06 – 1998/03 Austrian Armed Forces, Guard of Honor 3. Unit  
1989/09 – 1997/04 High School, Bundesrealgymnasium XII, Rosasgasse, Vienna  
1985/09 – 1989/06 Elementary school, Hermann-Brochgasse, Vienna

### ***Professional Experience:***

---

2006/01 – 2009/12  
PhD Thesis (Laboratory of Prof. Markus A. Rueegg)  
„Copine 6 a novel calcium sensor translating synaptic activity into spine plasticity“.  
Department of Neurobiology/Pharmacology, Biozentrum Basel, University of Basel

2005/01 – 2005/08  
Research Associate (Laboratory of Prof. J Nimpf)  
Institute of medical Biochemistry, University of Vienna

2003/06 – 2004/11  
Diploma Thesis: “The role of lipoprotein receptors in the antiphospholipid syndrome”.  
Vienna Bio Center, Max F. Perutz Laboratories, Institute of medical Biochemistry,  
Division of molecular genetics, University of Vienna

1998/07-1998/08  
Vienna International Airport, logistics and luggage claim

### ***Internship:***

---

2004/06/01 – 2004/06/23  
Laboratory of Prof. Phillip de Groot  
“Study of platelet adhesion to collagen after treatment with different lipoprotein receptor specific ligands.”  
Department of Haematology, Utrecht University Medical Center, Utrecht,  
The Netherlands

---

**Publications:**

---

**Sec24- and ARFGAP1-dependent trafficking of GABA transporter-1 is a prerequisite for correct axonal targeting.**

Reiterer V, Maier S, Sitte HH, **Kriz A**, Rüegg MA, Hauri HP, Freissmuth M, Farhan H. *J Neurosci*. 2008 Nov 19;28(47):12453-64.

**Signal-dependent export of GABA transporter 1 from the ER-Golgi intermediate compartment is specified by a C-terminal motif.**

Farhan H, Reiterer V, **Kriz A**, Hauri HP, Pavelka M, Sitte HH, Freissmuth M. *J Cell Sci*. 2008 Mar 15;121(Pt 6):753-61. Epub 2008 Feb 19.

---

**Languages:**

---

German: native (C2)  
English: fluent (C1)  
French: basics (A1)  
Spanish: basics (A1)

---

**References:**

---

Prof. Markus A. Rüegg; Principal Investigator;  
Department of Neurobiology/Pharmacology, Biozentrum, University of Basel

Prof. Dr. Johannes Nimpf; Principal Investigator;  
Vienna Bio Center, Max F. Perutz Laboratories, Department of medical Biochemistry,  
Biozentrum, University of Vienna

Prof. Philip G. de Groot; Principal Investigator;  
Department of Haematology, Utrecht University Medical Center, Utrecht,  
The Netherlands

---

The only way to discover the limits of the possible is to go beyond them into the impossible.

***Arthur C. Clarke***